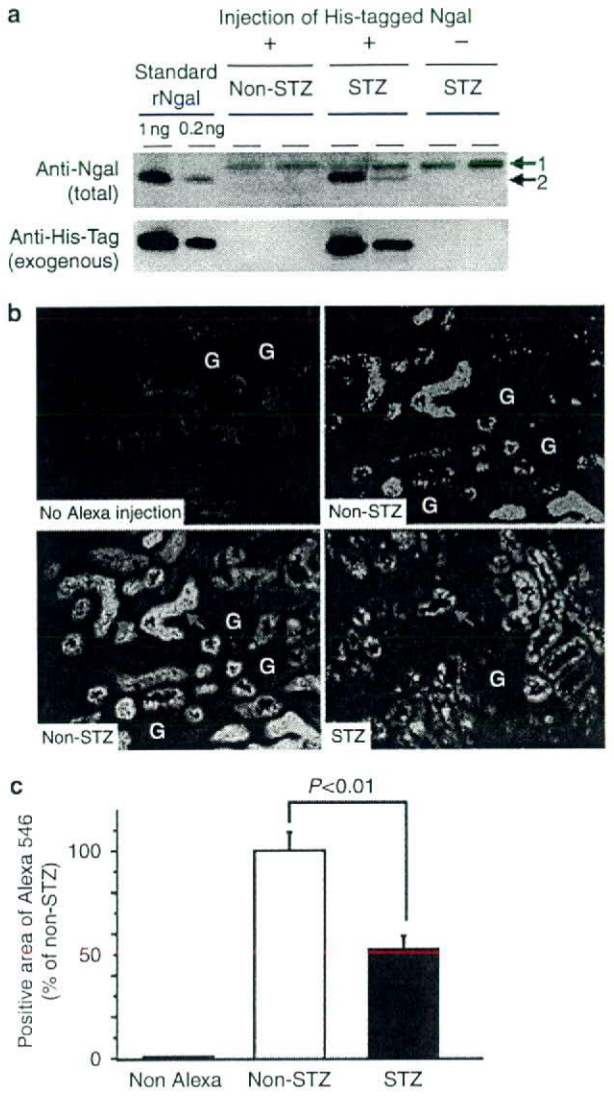

Figure 4 | Urinary excretion and tubular reabsorption of exogenously administered Ngal in STZ mice. (**a**) Western blot of urinary Ngal detected either with anti-Ngal or with anti-His-tag antibody at 8 weeks after induction of diabetes. Urine samples were collected for 12 h after His-tagged Ngal injection (i.p.) and 25 μl aliquots of them were separated by electrophoresis. Of note, STZ mice excreted much more diluted urine compared to non-STZ control mice. 1, endogenous Ngal (25 kDa, glycosylated); 2, His-tagged Ngal (21 kDa, unglycosylated). (**b**) Alexa Fluor 546-labeled Ngal was injected into STZ mice and kidneys were examined 30 min later. Arrows indicate Ngal protein distribution (in orange), which was homogeneous in non-STZ but was irregular and sparse in STZ mice. Top right panel shows selected area (in green) of positive fluorescence by computer software. G, glomeruli. Magnification, × 20. (**c**) Quantitation of exogenous Ngal uptake in kidneys of STZ and non-STZ mice ($n = 4$).

Urinary Ngal levels are highly elevated in human cases of nephrotic syndrome and are decreased in response to treatment

As cases of glomerular disorders with nephrotic syndrome, we investigated the clinical courses and changes in serum and urinary Ngal levels in human subjects. Case 1 was a 68-year-old woman with biopsy-proven minimal change disease. She had nephrotic range proteinuria (14 g/day) and gained body weight by 15 kg (from 62 to 77 kg) within 3 weeks. She was treated with i.v. steroid pulse (methyl prednisolone 1 g × 3 days), followed with oral prednisolone (beginning with 35 mg/day), and with three courses of hemodialysis on days 8, 9, and 12 after admission (Figure 6). Her proteinuria, edema, and azotemia resolved gradually. Concomitantly, urinary and serum Ngal levels decreased during the treatment, but reduction was much faster for urinary Ngal levels. There was a temporal elevation of urinary Ngal levels on day 21, which might reflect the reappearance of oligouria or proteinuria.

Case 2 was a 26-year-old woman, who was diagnosed to have membranous-type lupus nephritis (ISN/RPS class V). She was treated with two courses of i.v. steroid pulse, followed with oral prednisolone (Figure 6). Her urinary levels of protein and Ngal were decreased sharply within 17 days.

Case 3 was a 55-year-old woman with clinically diagnosed lupus nephritis (no biopsy). She had been treated with two courses of i.v. steroid pulse (1 g × 3 days) and oral prednisolone had been tapered from 50 to 35 mg/day, before changing the hospitals to ours. She was given i.v. cyclophosphamide pulse (0.4 g, once, 6 days after admission) and the immunosuppressant mizoribine (Asahi Kasei Pharma, Osaka, Japan; 100 mg/day). Urinary excretion of protein and Ngal decreased slowly (Supplementary Figure S1). Serum creatinine levels were constant throughout the course (0.4–0.5 mg/100 ml).

Case 4 was a 69-year-old man, who suffered from rapidly progressing, crescentic glomerulonephritis accompanied with moderate tubulointerstitial damage. His serum contained myeloperoxidase-type antineutrophil cytoplasmic antibody (MPO-ANCA, 138 EU). The maximum serum creatinine level was 5.6 mg/100 ml, and the proteinuria and azotemia responded slowly to treatment containing oral and i.v. steroid and i.v. cyclophosphamide (Supplementary Figure S1). Macrohematuria was observed, peaking at 5 days after cyclophosphamide administration. After 10 months, he showed signs of recurrence which were worsening in proteinuria, hematuria, azotemia, and MPO-ANCA titer (from < 10 to 37 EU). We observed reelevation of urinary Ngal levels during acute worsening of nephritis. Cyclosporine A (75 mg/day before breakfast) was added at 13 months, which appeared to support reduction of above mentioned signs.

To understand renal localization of Ngal protein in nephrotic patients, we carried out immunofluorescence study of renal biopsy samples and found close colocalization of signals of Ngal and albumin at the apical side of tubules. The results for case 1 are shown in Figure 7. These findings are consistent with those in animal experiments shown above (Figure 4), indicating highly active reabsorption of Ngal from glomerular filtrate.

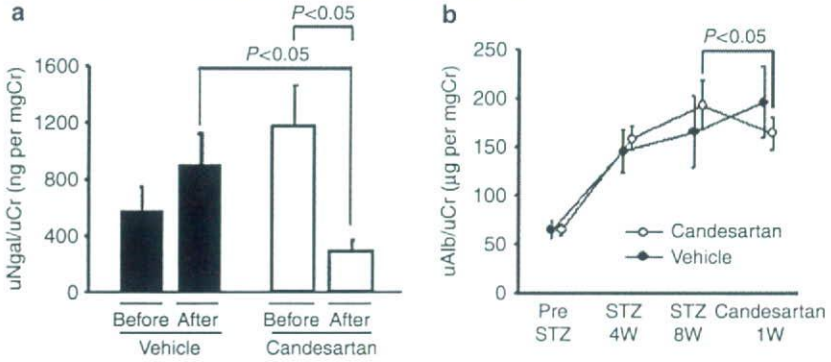

Figure 5 | Reduction of urinary Ngal and albumin excretion by candesartan in STZ mice. (**a**) Urinary Ngal (uNgal) and (**b**) albumin (uAlb) levels at 4 and 8 weeks after STZ injection and after one more week with candesartan (10 mg/kg/day, orally) or vehicle treatment ($n = 4$).

Table 1 | Blood glucose, urea nitrogen, creatinine levels, body weight, and blood pressure in STZ diabetic mice before and after candesartan treatment

	Vehicle		Candesartan	
	Before	After	Before	After
Blood glucose (mg/100 ml)	598 ± 2	593 ± 6	600 ± 3	591 ± 5
HbA1c (%)	11.7 ± 0.5	ND	12.5 ± 0.2	ND
Blood urea nitrogen (mg/100 ml)	ND	50 ± 2	ND	54 ± 1
Serum creatinine (mg/100 ml)	ND	0.13 ± 0.01	ND	0.11 ± 0.01
Body weight (g)	23.8 ± 0.9	23.5 ± 0.7	22.4 ± 0.5	22.8 ± 0.5
Systolic blood pressure (mm Hg)	104 ± 2	105 ± 0.9	103 ± 1	100 ± 1
Diastolic blood pressure (mm Hg)	55 ± 2	56 ± 1	50 ± 1	49 ± 2

Treatment with candesartan did not significantly alter these parameters. Blood urea nitrogen and serum creatinine levels in non-STZ control mice were 23 ± 3 and 0.09 ± 0.02 mg/100 ml, respectively. Blood was drawn when mice were fed *ad libitum*. ND, not determined.

In mice with obstructive nephropathy, Ngal protein is specifically located in the distal nephrons in the obstructed side by local synthesis, whereas it is confined to the proximal tubules in the contralateral side of the kidneys by reabsorption

As a model of post-renal kidney injury, we investigated mice with unilateral ureteral obstruction (UUO), in which distal nephrons are primarily affected, and studied the changes of Ngal protein levels in the obstructed and nonobstructed sides of the kidneys, serum, and urine (Figures 7 and 8). We also determined the renal distribution of Ngal by immunohistochemistry along with nephron segment markers: aquaporin (AQP) 1 for proximal tubules, Tamm-Horsfall protein (THP) for thick ascending limbs of Henle, and AQP 2 for collecting ducts (Figure 7; Figures S2–S4). In the UUO kidneys, after 1 day of ureter ligation, Ngal protein was expressed exclusively in thick ascending limbs of Henle, which was also expressing THP and was prominently dilated, suggesting that Ngal was synthesized in damaged epithelia. By striking contrast, in the contralateral kidneys, Ngal protein was confined to the apical side of aquaporin 1^+ proximal tubules. Ngal protein levels in the obstructed kidneys and in the urine from the dilated pelvis were continuously elevated for 2 weeks, whereas those in the nonobstructed kidneys and in the serum peaked at day 1 and decreased gradually. A smaller (17 kDa) fragment detected in the kidneys (but not in the urine and serum) using polyclonal anti-Ngal antibody may have been generated by lysosomal proteolysis of Ngal in the tubules.[2] Ngal mRNA expression was elevated by 100-fold in the obstructed kidneys (Figure 3), but it was only elevated by threefold in the contralateral kidneys at day 1 (data not shown). These findings indicate that Ngal was synthesized *de novo* in distal nephrons of obstructed kidneys, although it was highly but transiently accumulated in the serum, filtrated and reabsorbed in the contralateral kidneys.

In a case with interstitial nephritis, urinary Ngal levels decreased more rapidly than classic markers of tubular injury

Next, we investigated whether urinary Ngal is useful for evaluation of renal disorder with low-level proteinuria. Case 5 was a 25-year-old man, who was admitted to our hospital, presenting with general malaise, proteinuria (0.4 g/day), renal glucosuria and mild azotemia. He had taken an over-the-counter cold medicine 6 weeks earlier, and was positive in lymphocyte stimulation test for the drug. Renal biopsy revealed subacute interstitial nephritis with minor glomerular lesions. His signs and symptoms resolved by oral and i.v. prednisolone treatment. Table 2 and Figure S5 summarize the clinical course and changes in urinary biomarkers. The time to 50% reduction of urinary markers was in the order of Ngal $\leqslant$ (total) protein $<$ α1- and β2-microglobulins (classic markers of tubular proteinuria)

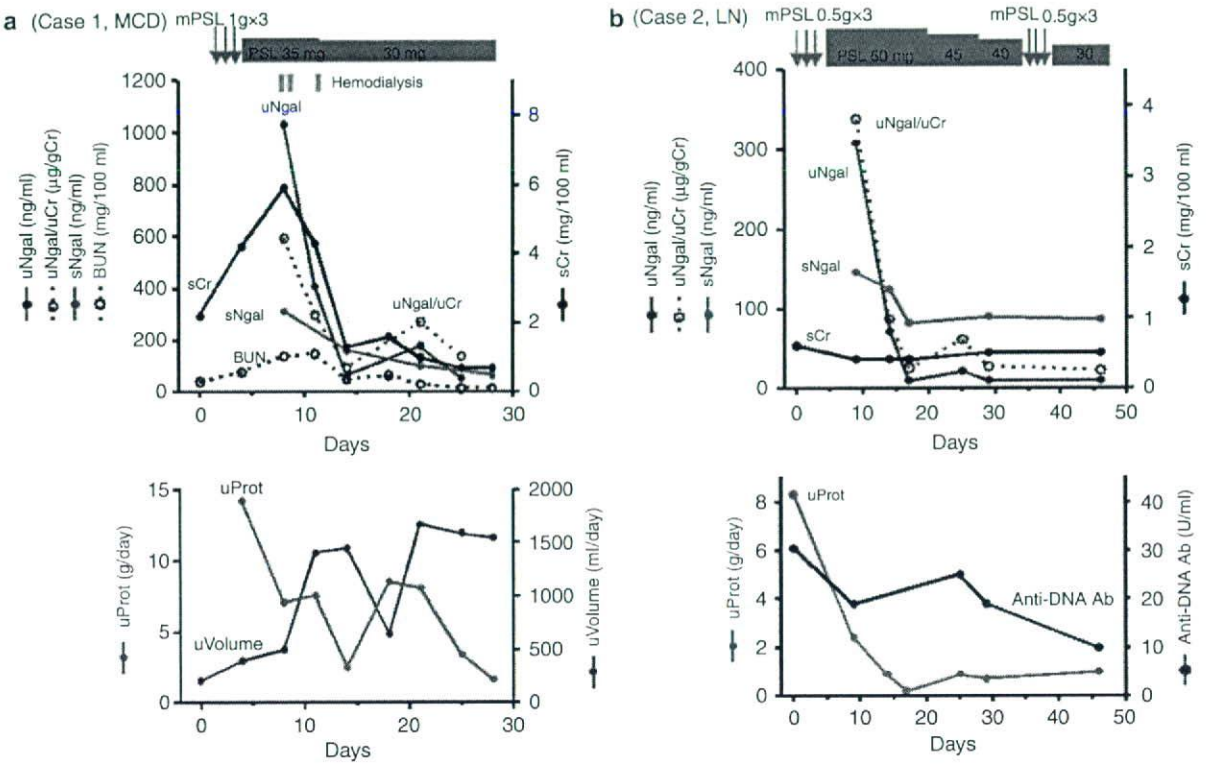

Figure 6 | Clinical course of 2 cases with nephrotic syndrome. (**a**) minimal change disease (case 1, MCD) and (**b**) lupus nephritis (case 2, LN). mPSL, methyl prednisolone; PSL, prednisolone; uProt, urinary protein excretion; sNgal, serum Ngal; uNgal, urinary Ngal; BUN, blood urea nitrogen; sCr, serum creatinine; uNgal/uCr, urinary Ngal normalized by urinary creatinine; Ab, antibody.

<*N*-acetyl-β-D-glucosaminidase. The fold-change during treatment was also largest in urinary Ngal, suggesting that urinary Ngal may be useful in monitoring the activity of nonglomerular renal disorders.

DISCUSSION

In the present study, we investigated urinary Ngal concentrations in patients with nephrotic syndrome (caused by acute and severe glomerular disorders) and interstitial nephritis and in mouse models of diabetic or obstructive nephropathy and found that the levels were unequivocally elevated (over 10-fold of control). In diabetic mice induced by STZ (as a model of slowly progressive chronic kidney disease), urinary Ngal appeared to derive mostly from impaired reabsorption in proximal tubules. In obstructed kidneys (as a model of post-renal AKI), Ngal was highly expressed in distal nephrons and accumulated in the urine collected from the pelvis. Therefore, STZ-diabetic and obstructed kidneys are the two extreme examples in which the primary source of urinary Ngal is glomerular filtrate and renal synthesis, respectively. In human renal disorders, urinary Ngal should be a mixture of these two major components. These findings indicate that in a variety of kidney diseases, urinary Ngal is a biomarker that can reflect damage in glomeruli, proximal tubules and distal nephrons.

Cross-sectional studies published so far have elucidated that urinary Ngal levels show certain correlation with urinary protein levels.[16,23] To our knowledge, this is the first human report to show very rapid and simultaneous reduction of urinary Ngal and protein concentrations by medical intervention. Surprisingly, the time course of urinary Ngal levels was associated to that of urinary protein levels not only in diabetic nephropathy and minimal change disease but also in crescentic glomerulonephritis and interstitial nephritis. In the latter disorders, treatment with steroid and immunosuppressant may have ameliorated Ngal reabsorption impairment and epithelial Ngal synthesis at the same time. The present findings suggest that urinary Ngal may be useful in the monitoring of disease activity and treatment efficacy. Of note, we cannot overgeneralize the findings in this study to all renal disorders, especially because we did not examine patients with severe, acute tubular necrosis, for instance, caused by renal ischemia or nephrotoxins (in which Ngal is abundantly synthesized by renal epithelia).[2]

In diabetic nephropathy, albumin excretion is increased by leakage from glomerular filtration barrier.[24] On the other hand, a number of reports elucidated the involvement of tubular dysfunction as a cause of albuminuria.[24–27] The size of Ngal protein (25 kDa) is smaller than albumin and, in normal conditions, Ngal is rapidly filtered by glomeruli and

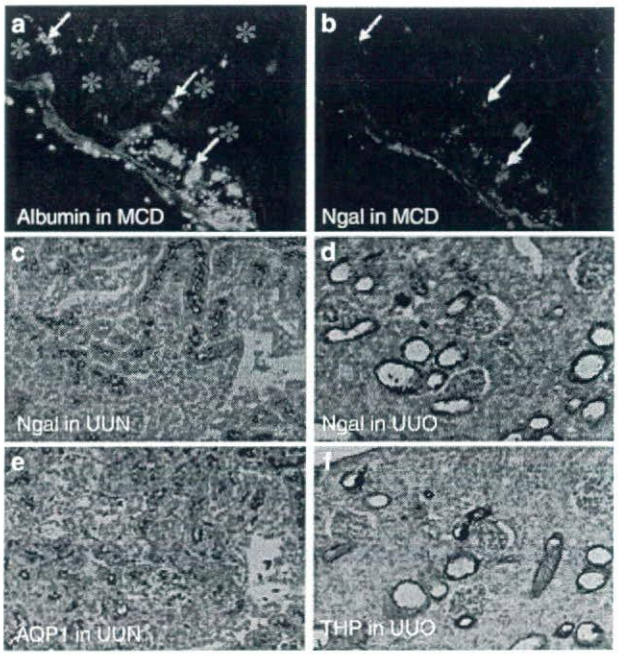

Figure 7 | Localization of Ngal protein expression in human and mouse kidneys. Immunofluorescence of (**a**, green) albumin and (**b**, red) Ngal in a patient with minimal change disease (MCD, magnification ×40). Arrows, colocalization of signals; asterisks, tubular lumen. Immunohistochemistry of (**c**, **d**) Ngal, (**e**) aquaporin 1 (AQP1), and (**f**) Tamm-Horsfall protein (THP) in the mouse kidney treated with (**d**, **f**) unilateral ureteral obstruction (UUO) and in the (**c**, **e**) contralateral kidney (UUN) at 1 day after operation (original magnification, ×20). Serial sections were analyzed.

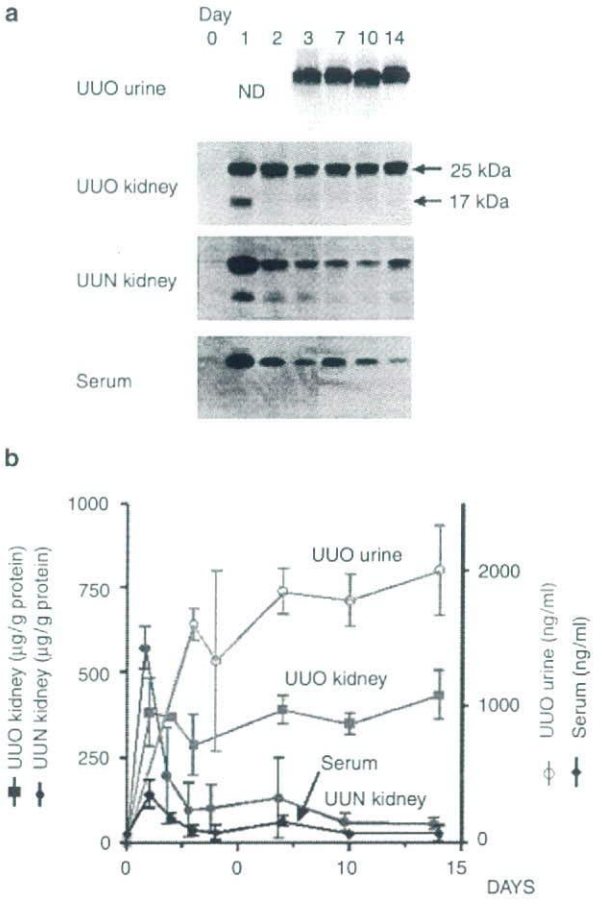

Figure 8 | Ngal protein levels in UUO, UUN, serum, and urine in mice with kidney obstruction. (**a**) Western blot analysis of Ngal protein. ND, not determined. (**b**) The mean Ngal concentrations in UUO, UUN, serum, and urine (collected from dilated pelvis of the UUO side using a needle and syringe). Elevation of Ngal concentrations were statistically significant at day 1 in UUO or UUN kidneys and serum, and at day 3 in urine ($P<0.01$ by unpaired t-test, $n=3$) compared to day 0 (no operation).

reabsorbed very efficiently by proximal tubules, leaving only 0.1–0.2% in the urine.[2] By analyzing renal handling of exogenously injected Ngal, the present study emphasized the existence of tubular reabsorption impairment in diabetic nephropathy.[28] In reverse, cellular stress in the proximal tubules may cause deterioration in diabetic nephropathy, as it was reported that transgenic overexpression of catalase in the proximal tubules of mice attenuated development of hypertension and albuminuria associating diabetic nephropathy.[29]

Treatment of STZ-diabetic mice with ARB significantly reduced urinary excretion of both Ngal and albumin. Two major scenarios can be proposed. First, ARB directly improved reabsorption efficiency in the proximal tubules, which may be mediated by increased peritubular capillary blood flow[30] and by amelioration of oxidative stress.[31] Second, ARB reduced intraglomerular hypertension and hyperfiltration,[32] reduced albumin leakage from glomeruli, and the total amount of the ligands for the common scavenger receptor megalin was decreased in the tubular lumen. This may increase the ratio of Ngal and albumin endocytosed at proximal tubules.

Here we used high-dose STZ to induce a model of diabetic nephropathy. Direct toxicity of STZ to proximal tubules may have exaggerated the elevation of urinary Ngal levels in these mice (which is 77-fold of control mice).[33] Hyperfiltration is reported in rodents given STZ.[32] In a previous report, threefold elevation in creatinine clearance was observed in C57BL/6 mice after treatment with STZ, but serum creatinine levels were not significantly decreased, likely due to concomitant osmotic diuresis and dehydration.[34] In the present study, hyperfiltration may have similarly occurred in STZ-diabetic mice. Growth arrest and leanness of STZ-diabetic mice may be partly related to selective reduction of serum Ngal levels (but not serum creatinine and BUN levels) in the present study, as obesity has been shown to be associated with elevated circulating Ngal levels.[35]

We also observed abundant urinary Ngal excretion in 4 patients with nephrotic syndrome. The mechanism may involve direct competition between Ngal and albumin at the surface of megalin molecule for receptor-mediated endocytosis[26,36] and also general malfunctioning of proximal tubules because of

Table 2 | Changes of urinary biomarker levels in case 5 (interstitial nephritis)

Days after admission	9	37	Fold difference[a]	Normal value
uNgal/uCr (μg/gCr)	256.6	25.4	10.1	<10 μg/l[b]
uProt/uCr (g/gCr)	0.381	0.052	7.3	<0.15 g/day
uβ2MG/uCr (mg/gCr)	18.2	2.8	6.5	<0.3 mg/l
uα1MG/uCr (mg/gCr)	46.4	17.2	2.7	<15 mg/l
sNgal (μg/l)	224	90	2.5	<106 μg/l[b]
uNAG/uCr (U/gCr)	21.1	8.7	2.4	<7 U/l
BUN (mg/100 ml)	15	11	1.4	<22 mg/100 ml
sCr (mg/100 ml)	1.2	1.0	1.2	<1.1 mg/100 ml[c]

MG, microglobulin; NAG, *N*-acetyl-β-D-glucosaminidase; Prot, protein; u and sNgal, urinary and serum Ngal; uCr, urinary creatinine.
[a]Fold difference between days 9 and 37.
[b]Value suggested by ELISA kit supplier.
[c]<1.1 for man and <0.8 for woman.

protein overload. Furthermore, a fraction of urinary Ngal may originate from renal synthesis in addition to reabsorption defect, but Ngal gene expression in human samples was not investigated in this study. The time required for urinary Ngal reduction was variable among cases: ranging from 2 weeks (cases 1 and 2) to more than a month (cases 3 and 4).

In a case with interstitial nephritis, urinary Ngal showed the largest fold increase and the quickest response to steroid treatment in comparison to other urinary biomarkers: total protein, α1- and β2-microglobulins and *N*-acetyl-β-D-glucosaminidase. These findings suggest that urinary Ngal might be particularly useful in the evaluation of kidney recovery in patients with low-grade proteinuria.

To summarize, urinary Ngal is a rapid biomarker of kidney injury and recovery showing a large fold-increase or decrease during clinical course of various renal disorders. Proteinuria seems to be one of important factors affecting Ngal'uria.

MATERIALS AND METHODS

Animal experiments

All animal experiments were conducted in accordance with our institutional guidelines for animal research. Male A-ZIP/F-1 heterozygous transgenic mice and control FVB/N littermates were used at 10 months of age, when A-ZIP/F-1 mice exhibit diabetic nephropathy with massive proteinuria.[18–20] Other animal experiments were carried out with male C57BL/6J mice (Japan Clea, Tokyo, Japan) starting at 8 weeks of age, when they weighted 21–23 g. Diabetes was induced by intraperitoneal injection of STZ (180 mg/kg of body weight; Sigma, St. Louis, MO, USA) in citrate buffer (pH 4.6) and control mice received only citrate buffer. Blood pressure was measured by the indirect tail-cuff method with MK-2000ST (Muromachi Kikai, Tokyo, Japan). Urine samples were collected with metabolic cages. Urinary albumin was measured with murine albumin ELISA (Exocell, Philadelphia, PA, USA). Serum and urinary creatinine levels were assayed by the enzymatic method (SRL, Tokyo, Japan). This method gives reliable measurement when compared to high-performance liquid chromatography method, even in low concentration materials, and performs much better than Jaffe's colorimetric method.[37] Blood glucose and HbA1c levels were determined in tail vein blood at *ad libitum*-fed conditions using Glutest Ace (Sanwa Kagaku, Nagoya, Japan) and DCA2000+ Analyzer (Bayer Medical, Tokyo, Japan), respectively. Mice were killed under pentobarbital anesthesia before organ collection. Prodrug of candesartan, candesartan cilexetil (TCV-116; Takeda Chemical Industries, Osaka, Japan), was initially dissolved at 10 mg/ml in a solution containing 16% polyethylene glycol no. 300 (vol/vol; Nacalai, Kyoto, Japan), 16% ethanol (Nacalai), and 0.7 M Na_2CO_3, and further diluted in drinking water to be given at a final dose of 10 mg/kg/day. This treatment method[38] gave less blood pressure lowering effects compared to gavage administration as previously described.[39] For UUO, mice were anesthetized with pentobarbital, the left kidney was exposed by midline incision, and the left ureter was ligated with 4–0 silk at two points.[40] Mice were killed 1–14 days after the operation.

Recombinant Ngal injection and detection

To investigate renal reabsorption of Ngal, 200 μg of 6 × histidine-tagged (at the C terminus) or 60 μg of Alexa Fluor 546 (Molecular Probes, Eugene, OR, USA)-labeled recombinant mouse Ngal (expressed in BL21 strain of *Escherichia coli*)[2] was injected into the peritoneum of mice. Urine samples were collected for 12 h after His-tagged Ngal injection. Urinary excretion of administered His-tagged Ngal was evaluated by Western blot analysis described below with anti-His antibody (MBL, Nagoya, Japan) or with goat polyclonal anti-mouse Ngal antibody (R&D Systems, Minneapolis, MN, USA). Kidneys were harvested 30 min after Alexa Fluor 546-labeled Ngal injection, snap frozen, sliced at 10 μm thickness and examined by a fluorescence microscope (IX81-PAFM; Olympus, Tokyo, Japan). The signal-positive areas were measured using MetaMorph 7.5 software (Molecular Devices, Downingtown, PA, USA).

Patients and measurement of human Ngal

Patients who admitted to Kyoto University Hospital for the diagnosis and treatment of renal disorders were enrolled under informed consent. This study was approved by the ethical committee on human research of Kyoto University Graduate School of Medicine. Ngal concentrations in the human serum and urine were determined by sandwich ELISA (AntibodyShop, Gentofte, Denmark) usually after 1000- and 250-fold dilution, respectively.

Western blot analysis

Urine, serum, and proteins extracted from organs were separated by SDS–polyacrylamide gel electrophoresis, transferred onto polyvinylidene difluoride membranes, incubated with primary antibody and detected with peroxidase-conjugated secondary antibody and

chemiluminescence. Serum was passed through 100-kDa cutoff membrane (Microcon YM-100; Millipore, Bedford, MA, USA) to remove immunoglobulins before analysis.[2] The amount of Ngal protein was measured by densitometry. Known amounts of recombinant mouse Ngal protein were used as standards.[2]

Real-time reverse transcription PCR

Total RNA was extracted from mouse kidneys and livers with TRIzol reagent (Invitrogen, Carlsbad, CA, USA) and cDNA in each sample was synthesized by High Capacity cDNA Reverse Transcription Kit (Applied Biosystems, Foster City, CA, USA). The mRNA levels of Ngal were determined using Premix Ex Taq (Takara Bio, Otsu, Japan) and ABI Prism 7300 Sequence Detector with the following primers and probe: Ngal forward, 5′-ggcagctttacgatgtacagca-3′; Ngal reverse, 5′-tctgatccagtagcgacagcc-3′; Ngal probe, 5′-FAM-catcctggt-cagggaccaggaccag-TAMRA-3′. Expression levels of Ngal were normalized by glyceraldehyde-3-phosphate dehydrogenase (internal control) levels, whose primer–probe set was purchased from Applied Biosystems.[41] Standard curve was made by serial dilution of cDNA from UUO kidneys.

Immunofluorescence of Ngal and albumin

Snap-frozen human biopsy samples were sliced at 3 μm thickness, fixed with acetone, and incubated with a solution containing both fluorescein isothiocyanate-labeled rabbit anti-human albumin antibody (Dako, Glostrup, Denmark) and goat polyclonal anti-human Ngal antibody (R&D Systems), followed by incubation with TexasRed-labeled anti-goat IgG (Jackson Immunoresearch, West Grove, PA, USA). The spillover of each signal was negligible.

Immunohistochemistry of Ngal and nephron markers

Mouse kidneys were fixed in 4% paraformaldehyde at 4 °C for 12 h and embedded in paraffin. Renal sections of 4 μm were deparaffined, hydrated, and incubated with 0.3% hydrogen peroxide. Antigen retrieval was performed by 0.05 mol/l citrate buffer (pH 6.0) for 10 min in a water bath heated at 100 °C (for Ngal, AQP1 and AQP2), or in a microwave oven (for THP). After cooling, the sections were incubated with 10% normal donkey or goat serum, followed by goat anti-mouse Ngal (1:300; R&D Systems), rabbit anti-AQP1 and AQP2 (1:200; Chemicon International, Temecula, CA, USA), or rabbit anti-THP antibodies (1:200; Biomedical Technologies, Stoughton, MA, USA). Primary antibodies were visualized with horseradish peroxidase-conjugated secondary antibodies and 3,3-diaminobenzidine tetrahydrochloride. Nuclei were counterstained with hematoxylin.

Statistical analysis

Results are expressed as mean ± s.e. Student's *t*-test was carried out to compare two groups. Statistical significance was defined as $P<0.05$.

DISCLOSURE

All the authors declared no competing interests.

ACKNOWLEDGMENTS

The authors are grateful to Dr O. Gavrilova and Dr M.L. Reitman (Diabetes Branch, NIDDKD, National Institutes of Health, Bethesda, MD, USA) for kindly providing A-ZIP/F-1 mice. We also acknowledge Ms Y. Ogawa, A. Yamamoto and other lab members for assistance. This work was supported by Astellas Foundation for Research on Metabolic Disorders, Kanae Foundation for the Promotion of Medical Science, Kurozumi Medical Foundation, Takeda Science Foundation, Smoking Research Foundation, Salt Science Research Foundation, and by Grant-in-Aid for Scientific Research of Japan Society for the Promotion of Science.

SUPPLEMENTARY MATERIAL

Figure S1. Clinical course of cases with (**a**) lupus nephritis (case 3, LN) and (**b**) crescentic glomerulonephritis (case 4, CrescGN).
Figure S2. Low-power fields showing expression of Ngal and nephron markers in unilateral ureteral obstruction (UUO) and contralateral kidneys.
Figure S3. High-power fields of cortex showing expression of Ngal and nephron markers in UUO and contralateral kidneys.
Figure S4. High-power fields of medulla showing expression of Ngal and nephron markers in UUO and contralateral kidneys.
Figure S5. Clinical course of a case with drug-induced interstitial nephritis (case 5, IntN).
Supplementary material is linked to the online version of the paper at http://www.nature.com/ki

REFERENCES

1. Mori K, Nakao K. Neutrophil gelatinase-associated lipocalin as the real-time indicator of active kidney damage. *Kidney Int* 2007; **71**: 967–970.
2. Mori K, Lee HT, Rapoport D *et al.* Endocytic delivery of lipocalin–siderophore–iron complex rescues the kidney from ischemia–reperfusion injury. *J Clin Invest* 2005; **115**: 610–621.
3. Barasch J, Mori K. Cell biology: iron thievery. *Nature* 2004; **432**: 811–813.
4. Yang J, Goetz D, Li JY *et al.* An iron delivery pathway mediated by a lipocalin. *Mol Cell* 2002; **10**: 1045–1056.
5. Mori K, Yang J, Barasch J. Ureteric bud controls multiple steps in the conversion of mesenchyme to epithelia. *Semin Cell Dev Biol* 2003; **14**: 209–216.
6. Flo TH, Smith KD, Sato S *et al.* Lipocalin 2 mediates an innate immune response to bacterial infection by sequestrating iron. *Nature* 2004; **432**: 917–921.
7. Schmidt-Ott KM, Mori K, Li JY *et al.* Dual action of neutrophil gelatinase-associated lipocalin. *J Am Soc Nephrol* 2007; **18**: 407–413.
8. Mishra J, Dent C, Tarabishi R *et al.* Neutrophil gelatinase-associated lipocalin (NGAL) as a biomarker for acute renal injury after cardiac surgery. *Lancet* 2005; **365**: 1231–1238.
9. Mishra J, Ma Q, Prada A *et al.* Identification of neutrophil gelatinase-associated lipocalin as a novel early urinary biomarker for ischemic renal injury. *J Am Soc Nephrol* 2003; **14**: 2534–2543.
10. Wagener G, Jan M, Kim M *et al.* Association between increases in urinary neutrophil gelatinase-associated lipocalin and acute renal dysfunction after adult cardiac surgery. *Anesthesiology* 2006; **105**: 485–491.
11. Bennett M, Dent CL, Ma Q *et al.* Urine NGAL predicts severity of acute kidney injury after cardiac surgery: a prospective study. *Clin J Am Soc Nephrol* 2008; **3**: 665–673.
12. Devarajan P. Emerging biomarkers of acute kidney injury. *Contrib Nephrol* 2007; **156**: 203–212.
13. Coca SG, Yalavarthy R, Concato J *et al.* Biomarkers for the diagnosis and risk stratification of acute kidney injury: a systematic review. *Kidney Int* 2008; **73**: 1008–1016.
14. Waikar SS, Bonventre JV. Biomarkers for the diagnosis of acute kidney injury. *Curr Opin Nephrol Hypertens* 2007; **16**: 557–564.
15. Nickolas TL, O'Rourke MJ, Yang J *et al.* Sensitivity and specificity of a single emergency department measurement of urinary neutrophil gelatinase-associated lipocalin for diagnosing acute kidney injury. *Ann Intern Med* 2008; **148**: 810–819.
16. Ding H, He Y, Li K *et al.* Urinary neutrophil gelatinase-associated lipocalin (NGAL) is an early biomarker for renal tubulointerstitial injury in IgA nephropathy. *Clin Immunol* 2007; **123**: 227–234.
17. Mitsnefes MM, Kathman TS, Mishra J *et al.* Serum neutrophil gelatinase-associated lipocalin as a marker of renal function in children with chronic kidney disease. *Pediatr Nephrol* 2007; **22**: 101–108.
18. Suganami T, Mukoyama M, Mori K *et al.* Prevention and reversal of renal injury by leptin in a new mouse model of diabetic nephropathy. *FASEB J* 2005; **19**: 127–129.

19. Moitra J, Mason MM, Olive M *et al.* Life without white fat: a transgenic mouse. *Genes Dev* 1998; **12**: 3168–3181.
20. Ebihara K, Ogawa Y, Masuzaki H *et al.* Transgenic overexpression of leptin rescues insulin resistance and diabetes in a mouse model of lipoatrophic diabetes. *Diabetes* 2001; **50**: 1440–1448.
21. Kjeldsen L, Johnsen AH, Sengeløv H *et al.* Isolation and primary structure of NGAL, a novel protein associated with human neutrophil gelatinase. *J Biol Chem* 1993; **268**: 10425–10432.
22. Brenner BM, Cooper ME, de Zeeuw D *et al.* RENAAL Study Investigators. Effects of losartan on renal and cardiovascular outcomes in patients with type 2 diabetes and nephropathy. *N Engl J Med* 2001; **345**: 861–869.
23. Bolignano D, Coppolino G, Campo S *et al.* Urinary neutrophil gelatinase-associated lipocalin (NGAL) is associated with severity of renal disease in proteinuric patients. *Nephrol Dial Transplant* 2008; **23**: 414–416.
24. Tucker BJ, Rasch R, Blantz RC. Glomerular filtration and tubular reabsorption of albumin in preproteinuric and proteinuric diabetic rats. *J Clin Invest* 1993; **92**: 686–694.
25. Tojo A, Onozato ML, Kurihara H *et al.* Angiotensin II blockade restores albumin reabsorption in the proximal tubules of diabetic rats. *Hypertens Res* 2003; **26**: 413–419.
26. Birn H, Christensen EI. Renal albumin absorption in physiology and pathology. *Kidney Int* 2006; **69**: 440–449.
27. Osicka TM, Houlihan CA, Chan JG *et al.* Albuminuria in patients with type 1 diabetes is directly linked to changes in the lysosome-mediated degradation of albumin during renal passage. *Diabetes* 2000; **49**: 1579–1584.
28. Chouinard S, Viau C. Reversibility of renal tubular dysfunction in streptozotocin-induced diabetes in the rat. *Can J Physiol Pharmacol* 1992; **70**: 977–982.
29. Brezniceanu ML, Liu F, Wei CC *et al.* Attenuation of interstitial fibrosis and tubular apoptosis in db/db transgenic mice overexpressing catalase in renal proximal tubular cells. *Diabetes* 2008; **57**: 451–459.
30. Manotham K, Tanaka T, Matsumoto M *et al.* Evidence of tubular hypoxia in the early phase in the remnant kidney model. *J Am Soc Nephrol* 2004; **15**: 1277–1288.
31. Onozato ML, Tojo A, Goto A *et al.* Oxidative stress and nitric oxide synthase in rat diabetic nephropathy: effects of ACEI and ARB. *Kidney Int* 2002; **61**: 186–194.
32. Zatz R, Dunn BR, Meyer TW *et al.* Prevention of diabetic glomerulopathy by pharmacological amelioration of glomerular capillary hypertension. *J Clin Invest* 1986; **77**: 1925–1930.
33. Breyer MD, Böttinger E, Brosius III FC *et al.* Mouse models of diabetic nephropathy. *J Am Soc Nephrol* 2005; **16**: 27–45.
34. Ichinose K, Maeshima Y, Yamamoto Y *et al.* Antiangiogenic endostatin peptide ameliorates renal alterations in the early stage of a type 1 diabetic nephropathy model. *Diabetes* 2005; **54**: 2891–2903.
35. Yan QW, Yang Q, Mody N *et al.* The adipokine lipocalin 2 is regulated by obesity and promotes insulin resistance. *Diabetes* 2007; **56**: 2533–2540.
36. Hvidberg V, Jacobsen C, Strong RK *et al.* The endocytic receptor megalin binds the iron transporting neutrophil-gelatinase-associated lipocalin with high affinity and mediates its cellular uptake. *FEBS Lett* 2005; **579**: 773–777.
37. Keppler A, Gretz N, Schmidt R *et al.* Plasma creatinine determination in mice and rats: an enzymatic method compares favorably with a high-performance liquid chromatography assay. *Kidney Int* 2007; **71**: 74–78.
38. Kosugi R, Shioi T, Watanabe-Maeda K *et al.* Angiotensin II receptor antagonist attenuates expression of aging markers in diabetic mouse heart. *Circ J* 2006; **70**: 482–488.
39. Shao J, Iwashita N, Ikeda F *et al.* Beneficial effects of candesartan, an angiotensin II type 1 receptor blocker, on beta-cell function and morphology in db/db mice. *Biochem Biophys Res Commun* 2006; **344**: 1224–1233.
40. Nagae T, Mori K, Mukoyama M *et al.* Adrenomedullin inhibits connective tissue growth factor expression, extracellular signal-regulated kinase activation and renal fibrosis. *Kidney Int* 2008; **74**: 70–80.
41. Yokoi H, Mukoyama M, Mori K *et al.* Overexpression of connective tissue growth factor in podocytes deteriorates diabetic nephropathy in mice. *Kidney Int* 2008; **73**: 446–455.

Circ J 2008; **72:** 1346–1350

Aldosterone, but Not Angiotensin II, Reduces Angiotensin Converting Enzyme 2 Gene Expression Levels in Cultured Neonatal Rat Cardiomyocytes

Megumi Yamamuro, MD; Michihiro Yoshimura, MD*; Masafumi Nakayama, MD; Koji Abe, MD; Hitoshi Sumida, MD; Seigo Sugiyama, MD; Yoshihiko Saito, MD**; Kazuwa Nakao, MD†; Hirofumi Yasue, MD††; Hisao Ogawa, MD

Background A previous report showed that aldosterone upregulates angiotensin converting enzyme (ACE) gene expression levels in cultured neonatal rat cardiocytes. ACE2 is a novel homologue of ACE, which exists in the human heart, and ACE2 converts angiotensin I to angiotensin 1–9 and angiotensin II to angiotensin 1–7, thereby decreasing angiotensin II levels. In the present study, an investigation took place to see whether aldosterone regulates the expression of ACE2 as well as that of ACE in cultured neonatal rat cardiomyocytes.

Methods and Results Primary neonatal rat cardiomyocytes were cultured with aldosterone. Total RNA was extracted from these cardiomyocytes and quantified the mRNA levels of ACE2, ACE and GAPDH by using real-time reverse transcription polymerase chain reaction analysis. Aldosterone significantly decreased ACE2 mRNA levels and increased ACE mRNA levels at 12 h. Angiotensin II, however, had no effect on either ACE2 mRNA levels or ACE mRNA levels. Eplerenone, a mineralocorticoid receptor antagonist, completely blocked the increase in ACE mRNA levels and the reduction in ACE2 mRNA levels due to aldosterone.

Conclusion Aldosterone, but not angiotensin II, reduced ACE2 mRNA levels and increased ACE mRNA levels in rat cardiomyocytes via mineralocorticoid receptor. Aldosterone might play an important role in cardiac remodeling by upregulating ACE and downregulating ACE2 levels. (*Circ J* 2008; **72:** 1346–1350)

Key Words: Heart failure; Hormones; Hypertrophy

It is now recognized that both angiotensin II and aldosterone play key roles in cardiac remodeling. We recently reported that aldosterone is secreted from the human heart in patients with heart failure or hypertension[1–3] We also reported that aldosterone, but not angiotensin II, upregulates angiotensin converting enzyme (ACE) gene expression levels in cultured neonatal rat cardiocytes, indicating that a positive feedback pathway from aldosterone to ACE might exist within the local cardiac rennin-angiotensin-aldosterone system[4]

Recently, ACE2, a novel homologue of ACE, has been cloned and identified; it has been reported that ACE2 gene expression occurs in the human heart[5–7] ACE2 is an essential regulator of heart function and is a strong candidate gene for hypertensive quantitative trait locus on the X chromosome[8] ACE converts angiotensin I to angiotensin II, which has a positive inotropic effect on the heart, but stimulates cardiomyocyte hypertrophy and interstitial fibrosis; however, when ACE2 intervenes between these cascades, it converts angiotensin I to angiotensin 1–9, by separating leucine. ACE and other enzymes subsequently cleave proline and phenylalanine to convert angiotensin 1–9 to angiotensin 1–7. ACE2 also directly and strongly converts angiotensin II to angiotensin 1–7 by separating phenylalanine[9–11] These cascades suggest that ACE2 would prevent cardiac remodeling by blocking angiotensin II generation. Furthermore, angiotensin 1–7, a product of ACE2 from angiotensin I or II, has cardio-protective effects. Indeed, it has been reported that angiotensin 1–7 reversed cardiac dysfunction, restored vascular endothelial responses and had anti-arrhythmic effects, and an ischemic effect caused significant increases in angiotensin 1–7 in myocytes within the non-infarcted regions of the cardiac ventricle[12–14] ACE2, which changes angiotensin II to angiotensin 1–7, could therefore be an important cardioprotective enzyme.

We hypothesized that aldosterone would directly regulate ACE2 gene expressions as well as ACE gene expressions by way of a minarelocorticoid receptor (MR). To investigate the direct action of aldosterone and angiotensin II, we used a purified neonatal rat cardiomyocyte culture system, which was independent of any hemodynamic overloads.

Methods

Agents Used in This Study

Aldosterone and angiotensin II were purchased from Steraloid Co (Wilton, NH, USA). Eplerenone, a mineralocorticoid receptor blocker, was provided by Pfizer Co, Ltd

(Received November 15, 2007; revised manuscript received March 11, 2008; accepted March 16, 2008)

*Department of Cardiovascular Medicine, Graduate School of Medical Sciences, Kumamoto University, Kumamoto, *Division of Cardiology, Department of Internal Medicine, The Jikei University School of Medicine, Tokyo, **First Department of Internal Medicine, Nara Medical University, Kashihara, †Department of Medicine and Clinical Science, Kyoto University Graduate School of Medicine, Kyoto and ††Division of Cardiology, Kumamoto Aging Research Institute, Kumamoto, Japan*
Mailing address: Michihiro Yoshimura, MD, Division of Cardiology, Department of Internal Medicine, The Jikei University School of Medicine, 3-25-8 Nishi-shinbashi, Minato-ku, Tokyo 105-8461, Japan.
E-mail: m.yoshimura@jikei.ac.jp

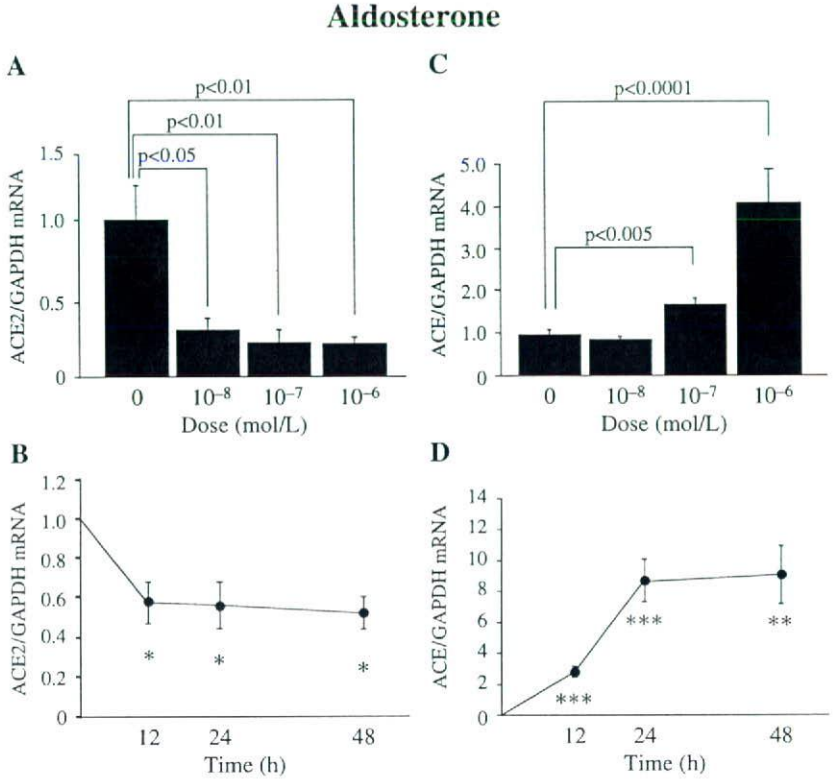

Fig 1. Effects of aldosterone on quantitative analysis of angiotensin converting enzyme (ACE) and ACE2 gene expression at various concentrations at 12 h and over time course. *p<0.05, **p<0.005, p<0.0005, n=9.

(New York, NY, USA).[15,16]

Preparation of Cardiomyocytes

All animal procedures were approved by the Animal Research Committee at Kumamoto University, and all procedures conformed to the National Institute of Health Guide for the Care and Use of Laboratory Animals. One- to 2-day-old Wistar rats were used for culturing cardiomyocytes. Ventricular cardiac cells were dispersed in a balanced sodium solution containing 0.04% collagenase II (Sigma, St. Louis, MO, USA) and 0.06% pancreatin (Sigma).[4,16,17] Cardiomyocytes were separately collected by a discontinuous Percoll gradient method using 40.5% and 58.5% Percoll (Sigma), which was prepared in the balanced sodium solution described above. Ventricular cells were suspended in the 58.5% layer of Percoll.[16,17] After centrifugation at 1,210 g for 30 min at 15°C, cardiomyocytes migrated to the discontinuous layer interface.

Cardiomyocyte Culture

Purified cardiomyocytes were plated at a density of 3.0×10^4 cells/cm^2 in 6-well plates (2.9×10^5 cells per well) in Dulbecco's modified Eagle's medium (DMEM, Gibco, Tokyo, Japan) supplemented with 10% fetal bovine serum (Moregate Bio Tech, Bulimba, Australia) and antibiotics (100 U/ml penicillin G and 100 μg/ml streptomycin; Gibco, New York, NY, USA). After 30 h of incubation, cardiomyocytes were maintained in serum-free DMEM for 12 h. After this preconditioning period, the culture was incubated in serum-free DMEM containing 1 mg/ml bovine serum albumin (Sigma) with the test substances.[16,17]

Isolation of Total RNA

Total RNA was extracted from cardiomyocytes cultured in 6-well plates using an RNeasy Mini Kit (Qiagen, Bulimba, Germany).[16,17] RNA was then treated with DNase I (Qiagen) to eliminate genomic DNA contamination.[16,17]

Design of Primers and Probes for Real-Time Reverse Transcription Polymerase Chain Reaction (RT-PCR) for Rat ACE, ACE2 and GAPDH

We used oligonucleotide primers and TaqMan probes for rat ACE2 and ACE, which were used as described.[4,18] Primers and the TaqMan probe for rat GAPDH were purchased from Perkin-Elmer Applied Biosystems (Foster City, CA, USA).

Quantitative Real-Time RT-PCR for Rat ACE, ACE2 and GAPDH

Two-step real-time RT-PCR was carried out with TaqMan Reverse Transcription Reagents (Applied Biosystems) and a TaqMan Universal Master Mix kit (Applied Biosystems)[19] using an ABI Prism 7700 sequence detection system (Applied Biosystems).[19]

Statistical Analysis

Data were expressed as means ± SEM. Statistical analysis was calculated using 1-way ANOVA followed by multiple comparisons using Fisher's protected least-significant difference and unpaired Student's t-test, as appropriate. $P<0.05$ was considered significant.

Results

Effects of Aldosterone on Quantitative Analysis of the ACE2 and ACE Gene Expressions

Aldosterone significantly decreased ACE2 mRNA levels at the time of 12 h (10^{-8} mol/L; 0.32±0.08-fold, 10^{-7} mol/L;

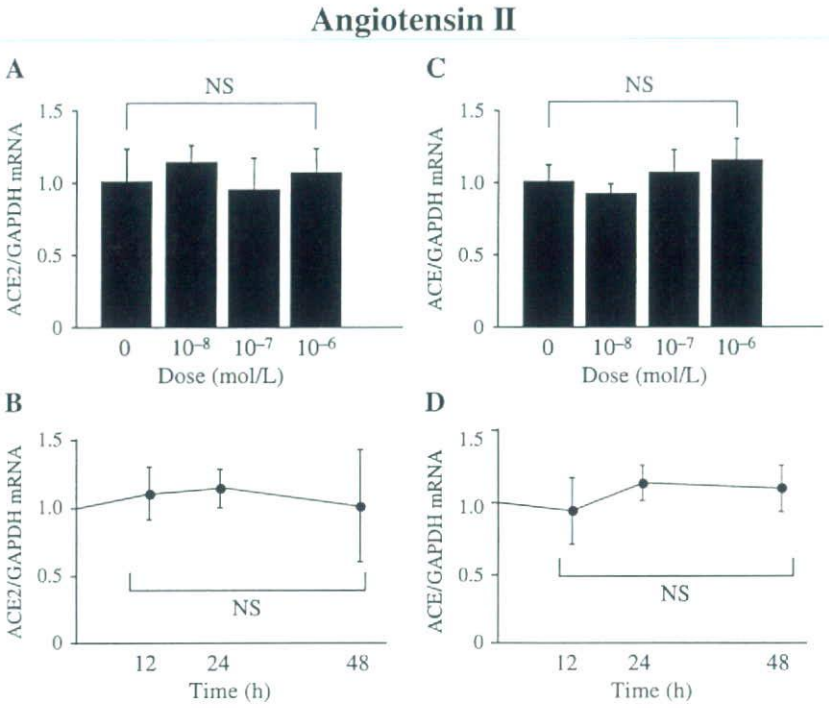

Fig 2. Effects of angiotensin II on quantitative analysis of angiotensin converting enzyme (ACE) and ACE2 gene expression at various concentrations at 12 h and over time course (n=9).

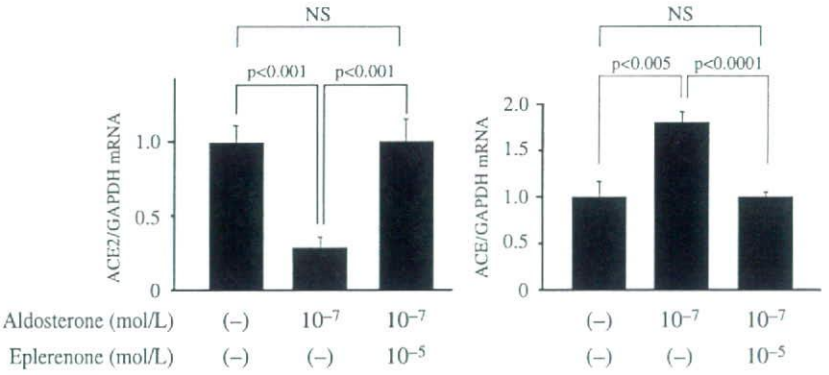

Fig 3. Effects of aldosterone and eplerenone on quantitative analysis of angiotensin converting enzyme (ACE) and ACE2 gene expression at 12 h (n=9).

0.23±0.09-fold and 10^{-6} mol/L; 0.22±0.04-fold compared with the control level, $p<0.05$, $p<0.01$ $p<0.01$, respectively, n=9). Aldosterone 10^{-7} mol/L significantly decreased the ACE2 mRNA level over time (12 h; 0.57±0.18-fold, 24 h; 0.55±0.21-fold and 48 h; 0.51±0.16-fold compared with the pre-treatment level, $p<0.05$, respectively, n=9) (Figs 1A and B).

However, aldosterone significantly increased ACE mRNA levels at the time of 12 h (10^{-7} mol/L;1.80±0.12-fold and 10^{-6} mol/L; 16.74±1.85-fold compared with the control level, $p<0.005$, $p<0.0001$, respectively, n=9). Aldosterone 10^{-7} mol/L significantly increased the ACE mRNA level over time (12 h; 3.70±0.34-fold, 24 h; 9.63±1.37-fold and 48 h; 9.98±1.87-fold compared with the pre-treatment level, $p<0.0005$, $p<0.0005$, $p<0.005$, respectively, n=9) (Figs 1C and D).

Effects of Angiotensin II on Quantitative Analysis of the ACE2 and ACE Gene Expressions

ACE2 and ACE gene expression levels with angiotensin II (10^{-6} mol/L, 10^{-7} mol/L and 10^{-8} mol/L) did not significantly change (n=9, Figs 2A and C). Furthermore, ACE2 and ACE gene expression levels with angiotensin II 10^{-7} mol/L did not significantly change over time (n=9, Figs 2B and D).

Effects of Aldosterone and Eplerenone on Quantitative Analysis of the ACE2 and ACE Gene Expressions at 12 h

Eplerenone completely blocked the reduction of the ACE2 gene expression and the increase of the ACE gene expression by aldosterone 10^{-7} mol/L at 12 h (Fig 3).

Discussion

Aldosterone promotes sodium retention acting at the distal tubules of the kidneys, thereby regulating both blood volume and blood pressure, and it has been implicated in the pathogenesis of heart failure.[20] Aldosterone causes blood pressure elevation[21] and, when combined with high salt intake, it produces cardiac hypertrophy, fibrosis, and/or vascular inflammatory injury;[22,23] however, the precise etiological role of aldosterone in the development of cardiac hypertrophy is not fully understood. In the current study, we showed

a possible cascade of a lot of mechanism in cardiac hypertrophy.

The present study shows that aldosterone 10^{-7} mol/L significantly reduced ACE2 gene expression levels until 12 h; however, aldosterone 10^{-7} mol/L significantly increased ACE gene expression levels until 24 h. These effects were completely blocked by eplerenone. Supposing eplerenone is a highly selective MR blocker[5,16] it is possible that aldosterone would genomically regulate ACE2 and ACE gene expression levels; therefore, aldosterone would play an important role in cardiac remodeling by instigating a vicious circle cascade by both downregulating ACE2 levels and upregulating ACE levels. Further investigation would be necessary to measure ACE2 and ACE protein levels in cardiomyocytes. These results lend credence to the fact that the blockade of aldosterone with either spironolactone or eplerenone might play an important role in improving the prognosis of patients with heart failure[24,25] It was reported that MR blockers reduced ACE2 expression in vivo studies[26–28]

We used a 10^{-7} mol/L dose of aldosterone, which is a close approximation to the in vivo situation, particularly under hyperaldosteronemic conditions. It has been reported, however, that aldosterone concentrations are one order higher in the cardiac tissues than in the peripheral circulation;[29] furthermore, we and others have shown that aldosterone is produced from the heart as well as from the adrenal glands in patients with heart failure, hypertension, or hypertrophic cardiomyopathy[1–3,29,30] Thus, aldosterone produced locally in the heart would probably activate myocardial MR in an autocrine or a paracrine manner in diseased states, such as cardiac hypertrophy or heart failure, aggravating the condition. In the present study, we suggested that 10^{-7} mol/L of aldosterone would act on downregulating ACE2 gene expression levels and upregulating ACE gene expression levels via MR in cultured neonatal rat cardiomyocytes. However, it is possible that high dose (10^{-6} mol/L) and more aldosterone might bring about these effects via gulucocorticoid receptor as well as via MR[31] This hypothesis has not yet to be tested and should be clear in another series of study.

In our data, angiotensin II did not act on ACE2 and ACE gene expression levels in cultured neonatal rat cardiomyocytes. However, it has been reported that angiotensin II receptor blocker up-regulated cardiac ACE2 gene expression levels and cardiac ACE2 activity in the heart by in vivo study using rats[32,33] It is thus seemingly a contradictory report for the present one. However, when considering that angiotensin II receptor blocker would inhibit aldosterone synthesis, the contradiction could be resolved. It is possible that angiotensin II might indirectly act on the ACE2 and ACE gene expression in the heart through aldosterone, which is activated in the adrenal gland, and is increased in the circulation level.

In conclusion, aldosterone, but not angiotensin II, reduced the gene expression levels of ACE2 and increased the gene expression levels of ACE in neonatal rat cardiomyocytes through MR and therefore instigated a vicious circler cascade in cardiac hypertrophy. Blockade of MR would be useful for the suppression of cardiac hypertrophy and ultimately for the prevention of heart failure.

Acknowledgements

This study was supported in part by grants-in-aid for the Ministry of Education, Culture, Sports, Science, and Technology, Tokyo [Young Scientists (B)-20790537 B (2)-15390248 and B (2)-15390249], the Ministry of Health, Labor and Welfare, Tokyo [14C-4, 14A-1, 17A-1 and 17C-2], the Smoking Research Foundation, Tokyo and Takeda Science Foundation, Tokyo, Japan.

Disclosure

We have no disclosures.

References

1. Mizuno Y, Michihiro Y, Yasue H, Sakamoto T, Ogawa H, Kugiyama K, et al. Aldosterone production is activated in failing ventricle in humans. *Circulation* 2001; **103:** 72–77.
2. Yamamoto N, Yasue H, Mizuno Y, Yoshimura M, Fujii H, Nakayama M, et al. Aldosterone is produced from the ventricles of patients with essential hypertension. *Hypertension* 2002; **39:** 958–962.
3. Yoshimura M, Nakamura S, Ito T, Nakayama M, Harada E, Mizuno Y, et al. Expression of aldosterone synthase gene in failing human heart: Quantitative analysis using modified real-time polymerase chain reaction. *J Clin Endocrinol Metab* 2002; **87:** 3936–3940.
4. Harada E, Yoshimura M, Yasue H, Nakagawa O, Nakagawa M, Harada M, et al. Aldosterone induces angiotensin-converting-enzyme gene expression in cultured neonatal rat cardiocytes. *Circulation* 2001; **104:** 137–139.
5. Donoghue M, Hsieh F, Baronas E, Godbout K, Gosselin M, Stagliano N, et al. A novel angiotensin-converting enzyme-related carboxypeptidase (ACE2) converts angiotensin I to angiotensin 1-9. *Circ Res* 2000; **87:** 1–9.
6. Tipnis SR, Hooper NM, Hyde R, Karran E, Christie G, Turner AJ. A human homolog of angiotensin-converting enzyme: Cloning and functional expression as a captopril-insensitive carboxypeptidase. *J Biol Chem* 2000; **275:** 33238–33243.
7. Burrell LM, Risvanis J, Kubota E, Dean RG, MacDonald PS, Lu S, et al. Myocardial infarction increases ACE2 expression in rat and humans. *Eur Heart J* 2005; **26:** 369–375.
8. Crackower MA, Sarao R, Oudit GY, Yagil C, Kozieradzki I, Scanga SE, et al. Angiotensin-converting enzyme 2 is an essential regulator of heart function. *Nature* 2002; **417:** 822–828.
9. Bernstein KE. Two ACEs and a heart. *Nature* 2002; **417:** 799–802.
10. Danilczyk U, Eriksson U, Crackower MA, Penninger JM. A story of two ACEs. *J Mol Med* 2003; **81:** 227–234.
11. Oudit GY, Crackower MA, Backx PH, Penninger JM. The role of ACE2 in cardiovascular physiology. *Trends Cardiovasc Med* 2003; **13:** 93–101.
12. Loot AE, Roks AJ, Henning RH, Tio RA, Suurmeijer AJ, Boomsma F, et al. Angiotensin-(1–7) attenuates the development of heart failure after myocardial infarction in rats. *Circulation* 2002; **105:** 1548–1550.
13. Ferreira AJ, Santos RA, Almeida AP. Angiotensin-(1–7): Cardioprotective effect in myocardial ischemia/reperfusion. *Hypertension* 2001; **38:** 665–658.
14. Averill DB, Ishiyama Y, Chappell MC, Ferrario CM. Cardiac angiotensin-(1–7) in ischemic cardiomyopathy. *Circulation* 2003; **108:** 2141–2146.
15. de Gasparo M, Joss U, Ramjoue HP, Whitebread SE, Haenni H, Schenkel L, et al. Three new epoxy-spirolactone derivatives: Characterization in vivo and in vitro. *J Pharmacol Exp Ther* 1987; **240:** 650–656.
16. Yamamuro M, Yoshimura M, Nakayama M, Abe K, Shono M, Suzuki S, et al. Direct effects of aldosterone on cardiomyocytes in the presence of normal and elevated extracellular sodium. *Endocrinology* 2006; **147:** 1314–1321.
17. Ito T, Yoshimura M, Nakamura S, Nakayama M, Shimasaki Y, Harada E, et al. Inhibitory effect of natriuretic peptides on aldosterone synthase gene expression in cultured neonatal rat cardiocytes. *Circulation* 2003; **107:** 807–810.
18. Tikellis C, Johnston CI, Forbes JM, Burns WC, Burrell LM, Risvanis J, et al. Characterization of renal angiotensin-converting enzyme 2 in diabetic nephropathy. *Hypertension* 2003; **41:** 392–397.
19. Kumar AP, Piedrafita FJ, Reynolds WF. Peroxisome proliferator-activated receptor gamma-ligands regulate myeloperoxidase expression in macrophages by an estrogen-dependent mechanism involving the -463GA promoter polymorphism. *J Biol Chem* 2004; **279:** 8300–8315.
20. Weber KT. Mechanisms of disease: Aldosterone in congestive heart failure. *N Engl J Med* 2001; **345:** 1689–1697.
21. Vasan RS, Evans JC, Larson MG, Wilson PWF, Meigs JB, Rifai N, et al. Serum aldosterone and the incidence of hypertension in nonhypertensive persons. *N Engl J Med* 2004; **351:** 33–41.

22. Ammarguellat FZ, Gannon PO, Amiri F, Schiffrin EL. Fibrosis, matrix metalloproteinases, and inflammation in the heart of DOCA-salt hypertensive rats: Role of ETA receptors. *Hypertension* 2002; **39:** 679–684.
23. Qin W, Rudolph AE, Bond BR, Rocha R, Blomme EAG, Goellner JJ, et al. Transgenic model of aldosterone-driven cardiac hypertrophy and heart failure. *Circ Res* 2003; **93:** 69–76.
24. Pitt B, Zannad F, Remme WJ, Cody R, Castaigne A, Perez A, et al. The effect of spironolactone on morbidity and mortality in patients with severe heart failure. *N Engl J Med* 1999; **341:** 709–717.
25. Pitt B, Remme W, Zannad F. Eplerenone, a selective aldosterone blocker, in patients with left ventricular dysfunction after myocardial infarction. *N Engl J Med* 2003; **348:** 1309–1321.
26. Karram T, Abbasi A, Keidar S, Golomb E, Hochberg I, Winaver J, et al. Effects of spironolactone and eprosartan on cardiac remodeling and angiotensin-converting enzyme isoforms in rats with experimental heart failure. *Am J Physiol Heart Circ Physiol* 2005; **289:** H1351–H1358.
27. Keidar S, Gamliel-Lazarovich A, Kaplan M, Pavlotzky E, Hamoud S, Hayek T, et al. Mineralocorticoid receptor blocker increases angiotensin-converting enzyme 2 activity in congestive heart failure patients. *Circ Res* 2005; **97:** 946–953.
28. Takeda Y, Zhu A, Yoneda T, Usukura M, Takata H, Yamagishi M. Effects of aldosterone and angiotensin II receptor blockade on cardiac angiotensinogen and angiotensin-converting enzyme 2 expression in Dahl salt-sensitive hypertensive rats. *Am J Hypertens* 2007; **20:** 1119–1124.
29. Silvestre JS, Robert V, Heymes C, Aupetit-Faisant B, Mouas C, Moalic JM, et al. Myocardial production of aldosterone and corticosterone in the rat. *J Biol Chem* 1998; **273:** 4883–4891.
30. Tsybouleva N, Zhang L, Chen S, Patel R, Lutucuta S, Nemoto S, et al. Aldosterone, through novel signaling proteins, is a fundamental molecular bridge between the genetic defect and the cardiac phenotype of hypertrophic cardiomyopathy. *Circulation* 2004; **109:** 1284–1291.
31. Hellal-Levy C, Couette B, Fagart J, Souque A, Gomez-Sanchez C, Rafestin-Oblin M. Specific hydroxylations determine selective corticosteroid recognition by human glucocorticoid and mineralocorticoid receptors. *FEBS Lett* 1999; **464:** 9–13.
32. Ishiyama Y, Gallagher PE, Averill DB, Tallant EA, Brosnihan KB, Ferrario CM. Upregulation of angiotensin-converting enzyme 2 after myocardial infarction by blockade of angiotensin II receptors. *Hypertension* 2004; **43:** 970–976.
33. Ferrario CM, Jessup J, Chappell MC, Averill DB, Brosnihan KB, Tallant EA, et al. Effect of angiotensin-converting enzyme inhibition and angiotensin II receptor blockers on cardiac angiotensin-converting enzyme 2. *Circulation* 2005; **111:** 2605–2610.

Adrenomedullin inhibits connective tissue growth factor expression, extracellular signal-regulated kinase activation and renal fibrosis

T Nagae[1], K Mori[1], M Mukoyama[1], M Kasahara[1], H Yokoi[1], T Suganami[1], K Sawai[1], T Yoshioka[1], M Koshikawa[1], Y Saito[1], Y Ogawa[1], T Kuwabara[1], I Tanaka[1], A Sugawara[1], T Kuwahara[2] and K Nakao[1]

[1]Department of Medicine and Clinical Science, Kyoto University Graduate School of Medicine, Kyoto, Japan and [2]Department of Nephrology, Osaka Saiseikai Nakatsu Hospital, Osaka, Japan

Systemic administration of the potent vasodilating peptide adrenomedullin reduces cardiac and renal fibrosis in hypertensive animals. Here, we investigated the effects of kidney-specific adrenomedullin gene delivery in normotensive rats after unilateral ureteral obstruction, an established model of renal tubulointerstitial fibrosis. Overexpression of exogenous adrenomedullin in the renal interstitium following ureteral obstruction significantly prevented fibrosis and proliferation of tubular and interstitial cells. In this model, there is upregulation of connective tissue growth factor (CTGF) mRNA expression and extracellular signal-regulated kinase (ERK) phosphorylation, and adrenomedullin overexpression suppressed both of these activities without altering the blood pressure. In NRK-49F renal fibroblasts, adrenomedullin reduced transforming growth factor-β-induced CTGF and fibronectin mRNA upregulation through the cyclic AMP/protein kinase A signaling pathway, and suppressed ERK phosphorylation and cell proliferation. In the kidneys with an obstructed ureter, adrenomedullin receptor gene expression was upregulated along with cyclic AMP production in kidney slices. The latter effect was partially blocked by a neutralizing antibody to adrenomedullin, indicating that an endogenous peptide-receptor system was activated. Our results show that overexpression of exogenous adrenomedullin in the ureteral-obstructed kidney prevents tubulointerstitial fibrosis and cell proliferation through the cyclic AMP-mediated decrease of CTGF induction and ERK phosphorylation.

Kidney International (2008) **74,** 70–80; doi:10.1038/ki.2008.98; published online 9 April 2008

KEYWORDS: TGF-β; cyclic AMP; gene expression; extracellular matrix; fibroblast

Correspondence: *K Mori, Department of Medicine and Clinical Science, Kyoto University Graduate School of Medicine, 54 Shogoin Kawahara-cho, Sakyo-ku, Kyoto 606-8507, Japan. E-mail: keyem@kuhp.kyoto-u.ac.jp*

Received 21 December 2006; revised 4 December 2007; accepted 3 January 2008; published online 9 April 2008

Tubulointerstitial fibrosis is a common feature of progressive renal injury and predicts the long-term outcome of renal function.[1] Among proposed mechanisms by which interstitial fibrosis progresses, transforming growth factor-β (TGFB1) plays a central role in the pathogenesis.[2–4] TGFB1 promotes the accumulation of extracellular matrix, through the enhanced synthesis of extracellular matrix proteins, such as fibronectin (FN1), and the inhibition of their degradation.[2] We have revealed that connective tissue growth factor (CTGF) is an important factor that mediates profibrotic action of TGFB1 in renal fibroblasts and in unilateral ureteral obstruction (UUO), an established model of obstructive nephropathy.[5,6] Introduction of *Ctgf* antisense oligonucleotide in the renal interstitium markedly suppresses renal fibrosis, but does not inhibit *Tgfb1* induction and cell proliferation in UUO.[6]

Adrenomedullin (ADM), a potent vasorelaxing and natriuretic peptide,[7] is expressed in renal glomeruli and tubules.[8,9] ADM exerts its actions by stimulating cyclic AMP (cAMP) production and by nitric oxide release in target tissues.[10–12] In humans, its receptor is composed of calcitonin receptor-like receptor (CRLR or CALCRL) and a family of receptor-activity-modifying proteins (RAMPs 1–3). RAMP2/CALCRL and RAMP3/CALCRL constitute ADM receptors, whereas RAMP1/CALCRL generates calcitonin gene-related protein (CGRP or CALCA) receptor.[13] We have reported that *Ramp1*, *Ramp2*, and *Calcrl* mRNAs are markedly upregulated after UUO in rats, and proposed that the ADM–RAMP system may modulate the process of tubulointerstitial fibrosis.[14] We and others have shown that ADM may either stimulate or inhibit cell proliferation, depending on the cell types. ADM has a proliferative action on 3T3 fibroblasts[15] and vascular smooth muscle cells,[16] but has an antiproliferative action on endothelial and mesangial cells,[10,17] and cardiac fibroblasts.[18] Systemic administration of ADM, in many cases, potently reduces blood pressure and exerts protective effects against cardiac and renal injury.[19–21] Heterozygotic *Adm*-deficient mice are predisposed to suffering from fibrotic changes in the cardiovascular system and in the kidney, indicating that endogenous ADM possesses organ protective

effects.[22–25] Whether local and direct action of ADM in the kidney is sufficient to prevent tubulointerstitial fibrosis and whether endogenous ADM–ADM receptor system is activated in obstructive nephropathy remains to be elucidated. In the present study, we investigated the effects of *ADM* overexpression in renal interstitium upon UUO. Furthermore, we examined the signaling pathway of ADM in the context of cAMP/protein kinase A (PKA), extracellular signal-regulated kinase (ERK or MAPK1/MAPK3), and also CTGF, which we have been proposing as a crucial profibrotic molecule acting downsteam of TGFB1 in obstructive nephropathy.[6] Finally, by *in situ* mRNA hybridization, we investigated the spatial regulation of ADM–ADM receptor system in UUO.

RESULTS

Renal fibrosis induced by UUO is prevented by exogenous expression of *ADM*

To investigate whether exogenous expression of *ADM* locally in the kidney ameliorates renal fibrosis induced by UUO, AxAM, an adenovirus encoding human *ADM* gene, was transferred into rat kidney via renal vein using hydrodynamics-based gene transfer technique.[6] Using control AxLacZ adenovirus injection, successful gene transfer was verified by positive X-gal staining specifically in interstitial cells of the obstructed kidney, and by the absence of expression in the other side of the kidney, liver, spleen, lung, and heart (Figure 1).[6,26] On day 6 after ureter ligation, exogenous human *ADM* mRNA expression was detected in AxAM-infected kidney (Figures 2 and 3). *In situ* hybridization revealed that human mRNA was indeed expressed predominantly in the interstitium, and expression in tubules was little, if any (Figure 2). In contrast, endogenous rat *Adm* was expressed in glomeruli and distal nephrons (presumably collecting ducts). UUO caused upregulation of rat *Adm* gene expression in inner medullary collecting ducts, but expression pattern in other parts of the kidney did not seem to be altered. These changes were reflected by slight elevation of rat *Adm* expression levels in the whole kidney (1.2-fold, but not significantly; Figure 3). Gene expression of *Tgfb1*, the key molecule involved in tissue fibrosis, was upregulated after UUO by 3.4-fold, and gene transfer of AxLacZ or AxAM did not affect the expression level. Gene expression of *Ctgf*, the critical factor that mediates profibrotic activity of TGFB1 in UUO,[5,6] was elevated in the obstructed kidney by 1.6-fold as compared with the sham-operated kidney. Introduction of AxAM into the kidney markedly inhibited *Ctgf* mRNA upregulation (by 75 ± 8%) compared with control AxLacZ adenovirus-treated obstructed kidney. Furthermore, gene expression of an extracellular matrix protein fibronectin (FN1) was upregulated in the obstructed kidney (4.2-fold of sham operation), and was significantly attenuated (by 81 ± 10%) with the transfer of AxAM. Immunohistochemical analysis revealed that FN1-expressing area was increased by 3.5-fold in UUO and was remarkably decreased in

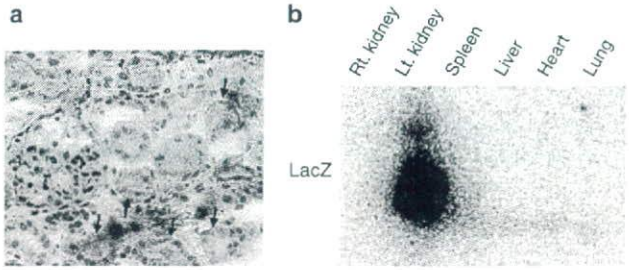

Figure 1 | Gene transfer into the rat kidney by hydrodynamics-based retrograde gene transfer via left renal vein. (**a**) X-gal staining (in blue) of the left kidney section at 6 days after transfection with AxLacZ reporter adenovirus. Arrows indicate the outer surfaces (basement membranes) of tubules. Original magnification × 200. (**b**) Expression of LacZ mRNA in various tissues analyzed by northern blotting.

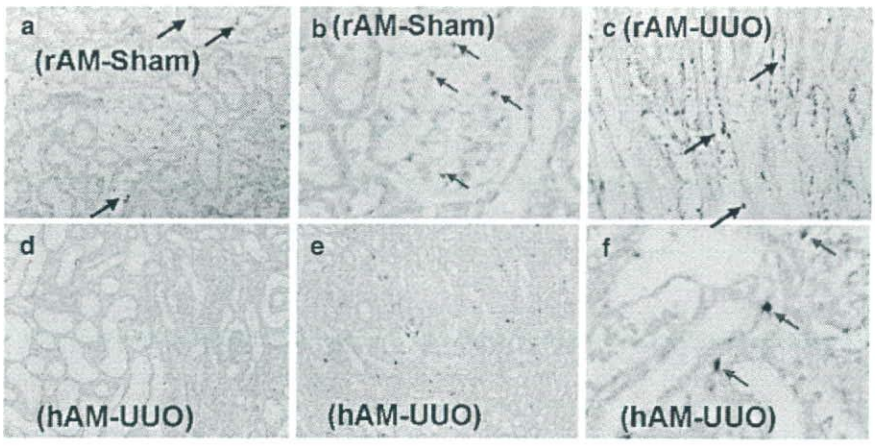

Figure 2 | Distribution of endogenous *Adm* and exogenous *ADM* in the rat kidney undergoing UUO. (**a**–**f**) *In situ* mRNA hybridization of the kidney on day 6 after ureter ligation. Gene expression of endogenous rat *Adm* (in dark blue staining, rAM) was detected in distal nephrons (**a**, black arrows) and glomeruli (**b**, red arrows) in sham-operated kidney, and was upregulated in inner medullary collecting ducts in UUO kidney (**c**, black arrows). By clear contrast, exogenous human *ADM* (hAM) was expressed in the interstitium of *ADM*-encoding adenovirus-treated obstructed kidney (**e**; **f**, blue arrows), but not in noninfected UUO kidney (**d**). Original magnification: × 100 (**d**, **e**), × 200 (**a**, **c**), and × 400 (**b**, **f**).

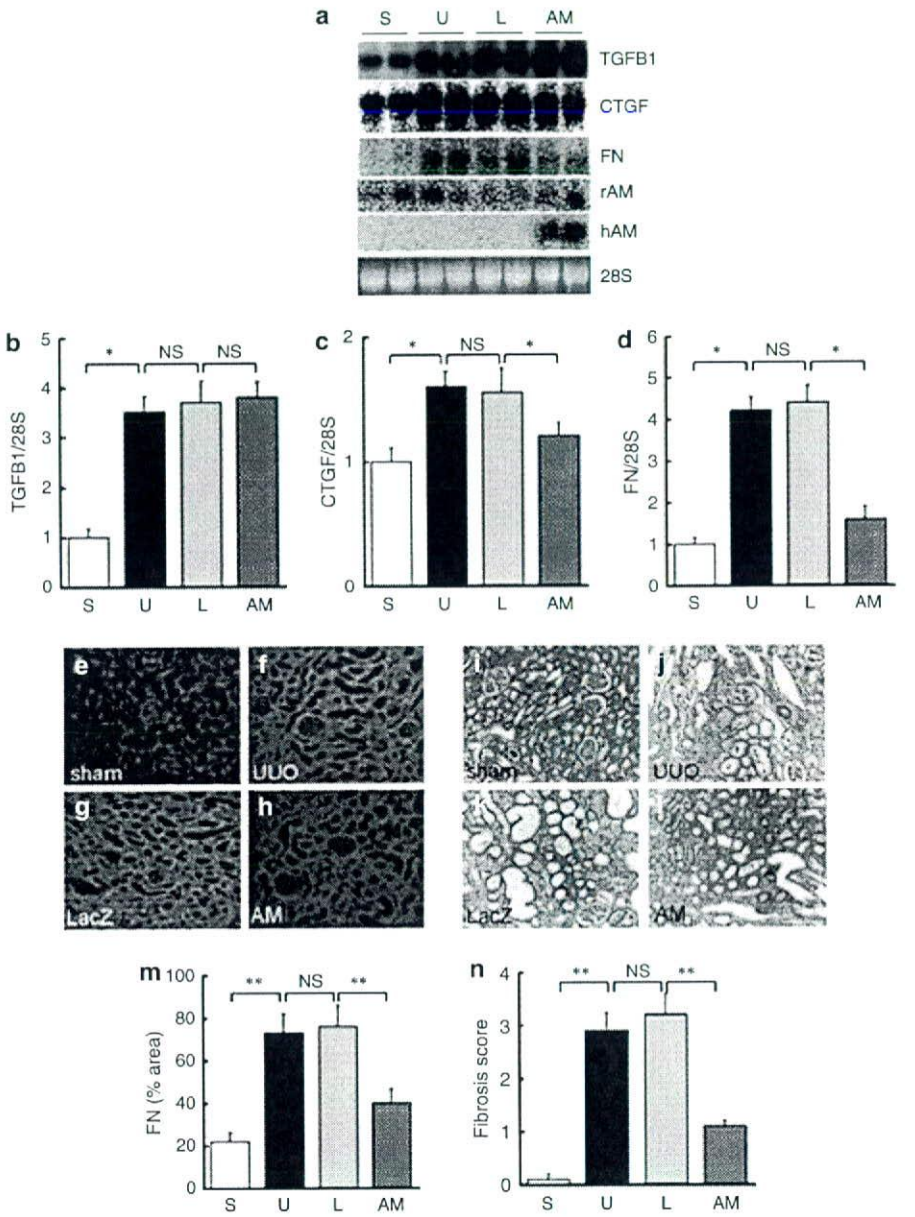

Figure 3 | Effects of *ADM* gene transfer in the rat kidney undergoing UUO. (**a–d**) Northern blot analysis of the kidney on day 6 after ureter ligation. S, sham-operated kidney; U, vehicle-treated ureter-ligated kidney; L, AxLacZ-treated obstructed kidney; AM, AxAM (*ADM*-encoding adenovirus)-treated obstructed kidney. The relative mRNA levels of *Tgfb1* (TGF-β), *Ctgf* (CTGF), and *Fn1* (FN) were normalized with 28S ribosomal RNA. rAM, rat *Adm*; hAM, human *ADM*. Mean levels of the sham-operated kidney from control rats were determined as 1.0 arbitrary unit. (**e–h, m**) Immunofluorescence staining of FN1 (FN) using fluorescein-conjugated antibody and quantified relative FN1$^+$ areas. (**i–l, n**) Fibrotic areas determined by Masson's trichrome staining (shown in blue) and semiquantitative scores of tubulointerstitial fibrosis. Original magnification × 200. *$P<0.05$; **$P<0.01$; NS, not significant; $n=5$ per each group.

AxAM-treated kidney (by 67 ± 9%). Furthermore, fibrosis score determined by Masson's trichrome staining was also elevated in AxLacZ-treated obstructed kidney compared with sham, and was significantly reduced in AxAM-treated kidney (the scores were 3.2 ± 0.4 for AxLacZ, 1.1 ± 0.1 for AxAM, and 0.1 ± 0.1 for sham). Urinary volume and systolic blood pressure measured by the tail-cuff method were not changed significantly after 6 days of UUO and by AxAM treatment (Figure 4). These observations show that exogenous *ADM* expressed in the renal interstitium inhibited renal fibrosis in UUO.

Cell proliferation after UUO is suppressed by exogenous expression of *ADM*

Because cellular proliferation of tubular and interstitial cells is one of the hallmarks of obstructive nephropathy, we carried out Western blot analyses for proliferating cell nuclear

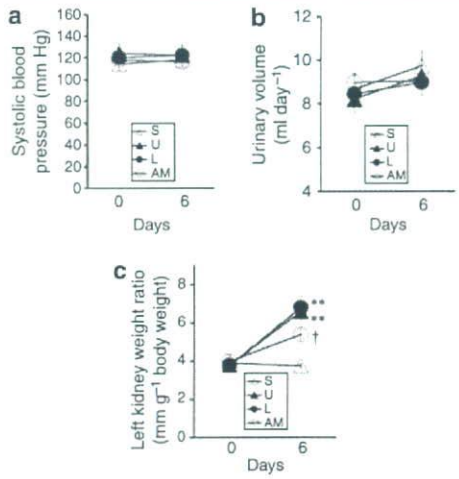

Figure 4 | Effects of ADM gene transfection on blood pressure, urinary volume, and kidney weight following renal obstruction in rats. (**a**) Systolic blood pressure. (**b**) Urinary volume. (**c**) Left kidney/body weight ratio. S, sham; U, vehicle treated UUO; L, AxLacZ-treated UUO; AM, AxAM-treated UUO. Mean ± s.e.m. $n = 5$; $^{**}P < 0.01$ vs each basal level; $\dagger P < 0.05$ vs U and L at day 6.

antigen (PCNA) and phosphorylated MAPK1/MAPK3, and immunostaining for PCNA. As shown in Figure 5, PCNA expression in the whole kidney was significantly increased after 6 days of ureter ligation, but upregulation of PCNA expression was significantly decreased in AxAM-treated kidney as compared with control AxLacZ-treated obstructed kidney (4.5- vs 9.6-fold of sham operation, respectively). Immunohistochemical study also indicated that the number of $PCNA^+$-proliferating cells in the obstructed kidney was increased both in the tubules and in the interstitium, and was decreased with *ADM* treatment. Cellular proliferation (Figure 5h and i) and extent of interstitial fibrosis (Figure 3m and n) were proportional to kidney weight/body weight ratio of the obstructed kidney (Figure 4c). Activation of MAPK1/MAPK3 plays an important role in tubular and interstitial cell proliferation.[27] The level of phosphorylated MAPK1/MAPK3 in whole kidney of AxLacZ-treated UUO rats was significantly increased (by 7.0-fold), compared with that in sham-operated kidney (Figure 5). AxAM treatment significantly suppressed MAPK1/MAPK3 phosphorylation in UUO (by 69 ± 13%). These findings indicate that renal cell proliferation during UUO was inhibited by *ADM* treatment, which may be due to reduced MAPK1/MAPK3 phosphorylation.

ADM inhibits TGFB1-induced *Ctgf* and *Fn1* upregulation through the cAMP/PKA signaling pathway

To address the molecular mechanism of *ADM*-mediated kidney protection in UUO, we examined direct actions of ADM on cultured NRK-49F normal rat renal fibroblasts. We investigated the effects of ADM on TGFB1-induced expression of CTGF and its downstream molecule FN1, both of which are critical mediators of tissue fibrosis.[5,6] *Ctgf* expression was strongly increased by TGFB1 in fibroblasts,

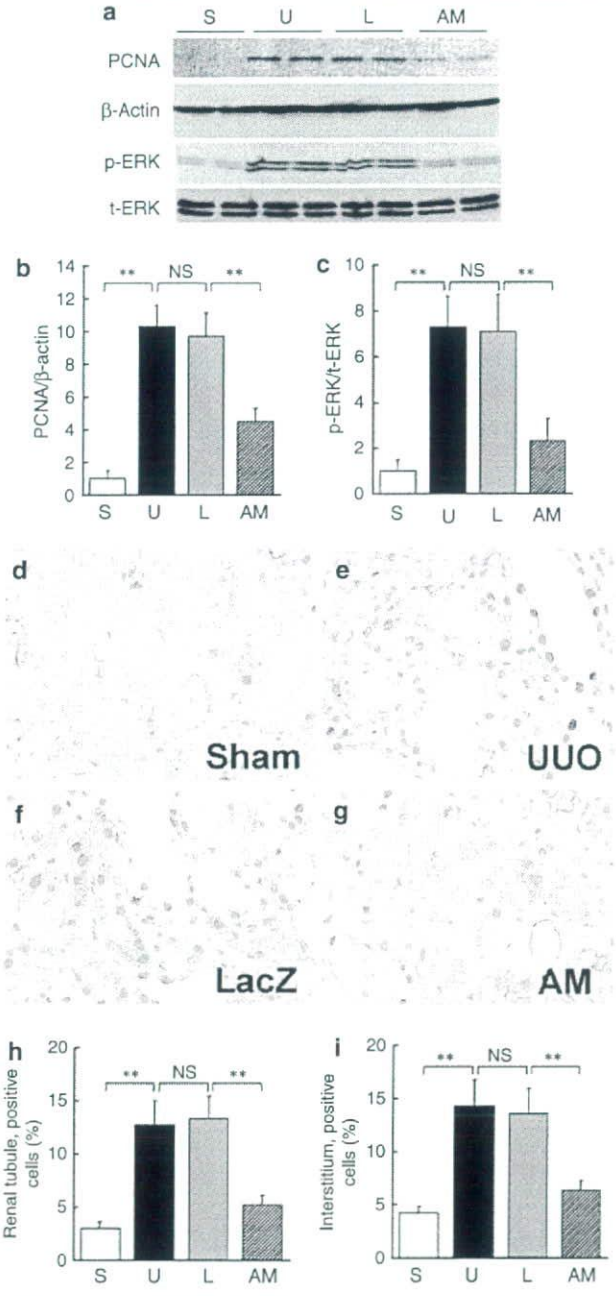

Figure 5 | PCNA expression and ERK (MAPK1/MAPK3) phosphorylation in the kidney of obstructive nephropathy. (**a**) Western blots of PCNA, β-actin, and phosphorylated and total MAPK1/MAPK3 (p-ERK and t-ERK) at day 6 after ureteral obstruction. Equal amounts of protein (40 μg per lane) from the whole kidney were separated by electrophoresis. S, Sham-operated kidney; U, vehicle-treated obstructed kidney; L and lacZ, AxLacZ-treated obstructed kidney; AM, AxAM-treated obstructed kidney. (**b**, **c**) The relative levels of PCNA/β-actin and p-ERK/t-ERK measured with densitometer. (**d**–**g**) Immunohistochemistry for PCNA (stained in brown) in the obstructed kidney. Original magnification × 400. All the nuclei were further visualized with hematoxylin counterstaining for quantification (not shown). (**h**, **i**) The ratio of $PCNA^+$ cells in renal tubular and interstitial cells. $^{**}P < 0.01$, NS, not significant; $n = 5$.

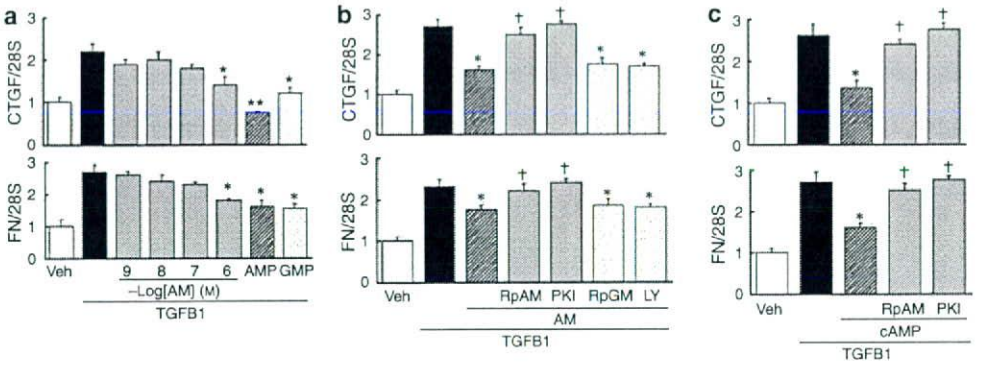

Figure 6 | Antifibrotic effects of ADM upon NRK-49F normal rat kidney fibroblasts. (**a**) Northern blot analysis of TGFB1 (3 ng ml^{-1})-induced upregulation of *Ctgf* and *Fn1* gene expression, and suppression by ADM (AM, final 10^{-9}–10^{-6} M) and by 8-bromo-cAMP and 8-bromo-cGMP (AMP and GMP, 1 mM each). Veh, vehicle. (**b**) Effects of protein kinase inhibitors upon the antifibrotic actions of ADM (AM, 1 μM). Rp-cAMP (RpAM, 10 μM) and myristoylated protein kinase A inhibitor amide 14–22 (PKI, 0.5 μM) are inhibitors for PKA; RpGM, protein kinase G inhibitor Rp-cGMP (10 μM); LY, phosphatidylinositol 3-kinase inhibitor LY29400 (10 μM). (**c**) cAMP/PKA-dependent inhibition of TGFB1-induced fibrotic changes. *$P<0.05$, **$P<0.01$ vs TGFB1 alone; †$P<0.05$ vs TGFB1 + ADM/cAMP, $n=6$.

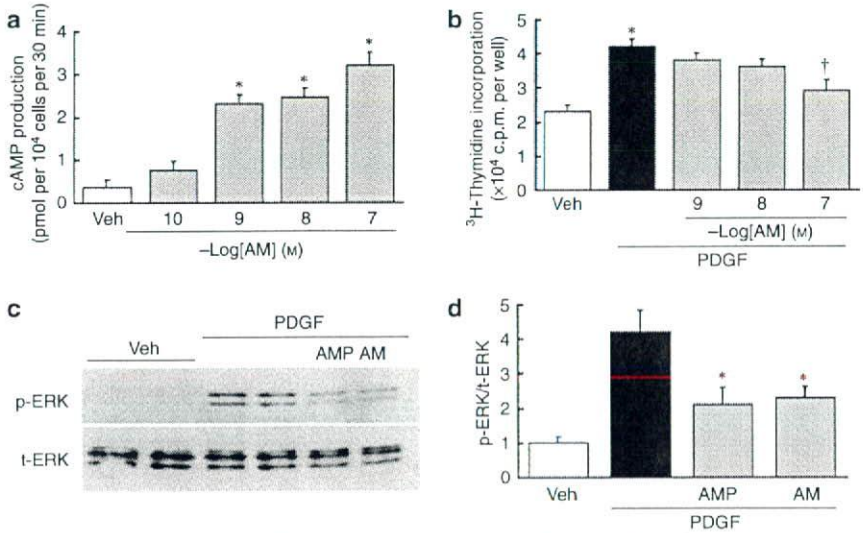

Figure 7 | Antiproliferative effects of ADM upon NRK-49F cells. (**a**) ADM (AM, final 10^{-10}–10^{-7} M)-stimulated increase of cAMP production. Veh, vehicle. *$P<0.05$ vs vehicle. (**b**) Inhibitory effects of ADM upon PDGF-BB (PDGF, 3 ng ml^{-1})-stimulated ^{3}H-thymidine incorporation. *$P<0.05$ vs vehicle, †$P<0.05$ vs PDGF alone, $n=6$. (**c**, **d**) Inhibitory effects of ADM upon MAPK1/MAPK3 phosphorylation. ADM (AM, 1 μM) and cAMP analog (AMP, 1 mM) significantly inhibited PDGF (3 ng ml^{-1})-induced phosphorylation of MAPK1/MAPK3. p, phosphorylated; t, total. Equal amounts of protein (40 μg per lane) were subjected to Western blot analysis. *$P<0.05$ vs PDGF alone, $n=4$.

and pretreatment with ADM dose dependently inhibited TGFB1-induced *Ctgf* mRNA upregulation (Figure 6). Because cAMP and cyclic GMP (cGMP) are major intracellular signaling molecules for ADM action, we examined whether they can substitute for ADM as to suppression of *Ctgf* induction. Membrane-permeable analogs of cAMP and cGMP (8-bromo-cAMP and 8-bromo-cGMP) both effectively abolished the upregulation of *Ctgf* gene expression. Essentially, similar results were obtained on *Fn1* gene expression. These findings raised the possibility that ADM inhibits TGFB1-induced *Ctgf* and *Fn1* upregulation through cAMP, cGMP, or both. Therefore, we examined which of cAMP and cGMP is the predominant mediator of the antifibrotic action of ADM. Pretreatment with PKA inhibitors, Rp-cAMP (adenosine 3′,5′-cyclic monophosphorothioate) and myristoylated PKA inhibitor amide 14–22, canceled ADM-induced inhibition of *Ctgf* and *Fn1* upregulation (Figure 6). By contrast, protein kinase G inhibitor Rp-cGMP (guanosine 3′,5′-cyclic monophosphorothioate) and phosphatidylinositol 3-kinase inhibitor LY294002 had no significant effects. In control experiments, both PKA inhibitors reversed inhibitory effects of cAMP itself on TGFB1-induced *Ctgf* and *Fn1* mRNA upregulation. Finally, ADM stimulated intracellular cAMP production in NRK-49F cells (Figure 7a). These findings show that the antifibrotic effects of ADM in cultured renal fibroblasts were mediated mainly through the cAMP/PKA cascade.

ADM suppresses proliferation and MAPK1/MAPK3 phosphorylation of renal fibroblasts

Adrenomedullin has a proliferative action on 3T3 fibroblasts[15] and vascular smooth muscle cells,[16] but has an antiproliferative action on endothelial and mesangial cells.[10] We examined the effects of ADM on renal fibroblast proliferation. ADM inhibited platelet-derived growth factor (PDGF)-BB-induced DNA synthesis in a dose-dependent fashion (Figure 7). Next, we examined the effects of ADM on MAPK1/MAPK3 phosphorylation, as MAPK1/MAPK3 phosphorylation plays a key role in the induction of interstitial cell proliferation.[27] Preincubation with ADM or a membrane-permeable cAMP analog significantly inhibited PDGF-induced MAPK1/MAPK3 phosphorylation (Figure 7). These results indicate that ADM inhibited MAPK1/MAPK3 phosphorylation and renal fibroblast proliferation.

cAMP production is augmented in UUO kidney, partially by endogenous ADM

In this study, we have demonstrated that exogenous *ADM* inhibits *Ctgf* and *Fn1* upregulation and cell proliferation in UUO kidney and in cultured renal fibroblasts, and that cAMP plays a crucial role in these ADM actions. Using cAMP as a reporter, we investigated whether the endogenous ADM–ADM receptor system is activated in UUO. Basal cAMP production of renal tissue slices from whole kidney was increased by 2.4-fold in UUO compared with control (Figure 8). This was also true when the medulla, cortex, or glomeruli was examined separately. Addition of ADM increased cAMP production in the medulla and glomeruli from control and UUO rats, indicating the presence of active ADM receptors. To evaluate the contribution of endogenous ADM in enhanced rate of cAMP production in UUO kidney, ADM-neutralizing antibody was added to renal tissue slices. Basal cAMP production in control kidney was not affected significantly by ADM-neutralizing antibody (Figure 8). In contrast, the antibody partially inhibited cAMP elevation in whole kidney, medulla, cortex, and glomeruli from UUO rats. As a control, control ascites gave no effects. These findings indicate that the endogenous ADM–ADM receptor system was activated in UUO kidney.

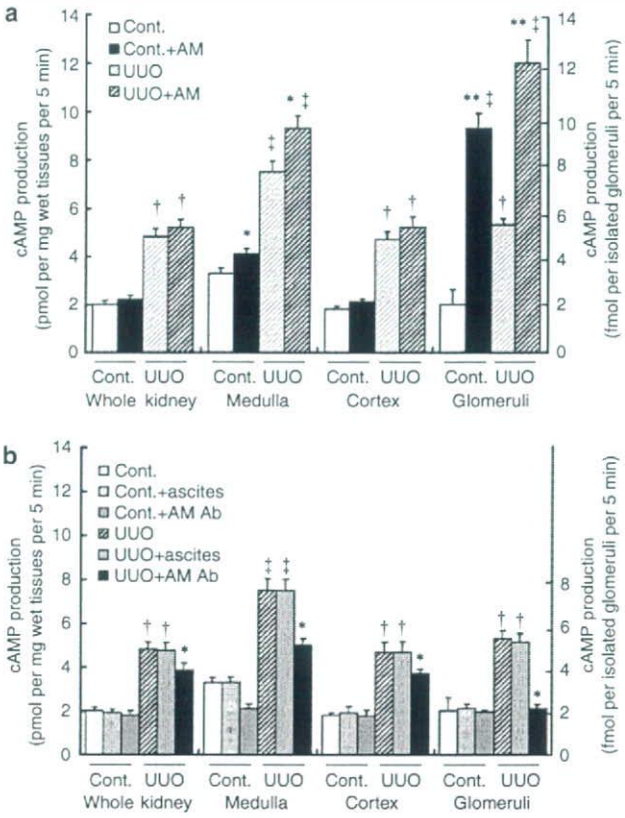

Figure 8 | Effects of ADM upon cAMP production rate in kidney tissue slices and in isolated glomeruli from UUO rats. (**a**) Basal and ADM (AM)-induced cAMP production. (**b**) Blockade of cAMP production by neutralizing ADM (AM) antibody. †$P<0.05$, ‡$P<0.01$ vs basal (ADM-untreated conditions) of control (non-UUO kidney); *$P<0.05$, **$P<0.01$, significant changes by ADM (**a**) or by neutralizing ADM antibody treatment (**b**); $n=6$.

Transient coexpression of *Calcrl* (CRLR) and *Ramp2* or *Ramp3* generate ADM receptor, and *Calcrl* and *Ramp1* generate CALCA (CGRP) receptor

In humans and mice, functional reconstitution of RAMPs 1–3 and CALCRL as ADM or CALCA receptor has been reported.[13,28–30] To clarify the rat ADM receptor selectivity, we made expression vectors for rat *Ramp's* and *Calcrl* and transfected them into COS-7 cells. As shown in Figure 9, when *Ramp2* or *Ramp3* was co-transfected with *Calcrl*, ADM markedly increased cAMP production, but when *Ramp1* and *Calcrl* was co-transfected, ADM induced little cAMP production. In contrast, only when *Ramp1* was co-transfected with *Calcrl*, CALCA markedly increased cAMP production (Figure 9). These results indicate that similarly to human counterparts, transient coexpression of rat *Calcrl* and *Ramp2* or *Ramp3* generated the receptors specific to ADM, and that *Calcrl* and *Ramp1* generated the CALCA receptor.

Ramp2 and *Ramp1* are upregulated in renal medulla, cortex, and glomeruli after UUO

To further characterize the role of RAMPs 1–3 in UUO, we analyzed their renal distribution and the change of expression. Northern blot analyses revealed that *Ramp1* was mainly upregulated in medulla and cortex, *Ramp2* in medulla, cortex, and glomeruli at 6 days after UUO, whereas *Ramp3* was unchanged (Figure 10). Through all these *in vivo* and *in vitro* experiments, it is suggested that upregulation of *Ramp2* expression activated the ADM–ADM receptor system in UUO kidney.

Ramp1 is expressed in all nephron segments, upregulated evenly, and newly induced in interstitium after UUO

Finally, we investigated renal distribution of *Ramp2* gene expression before and after UUO (Figure 11). *In situ* hybridization revealed that *Ramp2* was expressed in virtually all nephron segments including glomeruli in sham-operated

kidney. Especially, distal nephrons (such as thick ascending limbs of Henle and collecting ducts) expressed *Ramp2* abundantly. After UUO, *Ramp2* gene expression was enhanced evenly in nephron segments. At the same time, *de novo* expression was induced in interstitium adjacent to dilated distal nephrons. These findings suggest that renal interstitium was an important target of endogenous and exogenous ADM in the present study.

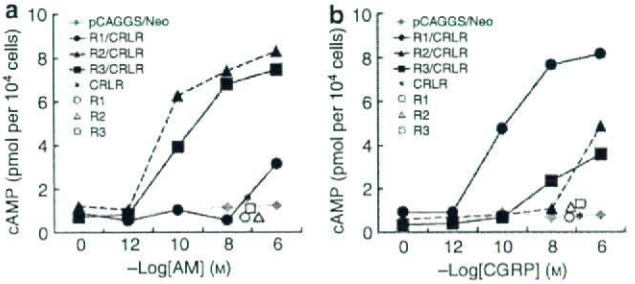

Figure 9 | Cyclic AMP production in COS-7 cells overexpressing *Ramps 1–3* and/or *Calcrl* (*CRLR*). ADM (**a**, AM) or CALCA (**b**, CGRP)-induced cAMP production. pCAGGS/Neo, mock; R1-R3, *Ramps 1–3*. Average of $n = 4$.

DISCUSSION

In the present study, we locally overexpressed exogenous *ADM* predominantly in the renal interstitial cells in obstructed nephropathy by injecting *ADM*-encoding adenovirus via renal vein, and revealed the protective action of ADM, which was characterized with suppression of interstitial fibrosis and of cellular proliferation. Administration of *ADM* adenovirus also caused downregulation of CTGF, FN, PCNA, and phosphorylation of MAPK1/MAPK3 in the kidney. Unlike systemic delivery of the *Adm* gene[19,20] or administration of ADM[21] in previous reports, we did not observe blood pressure reduction in our model, highlighting the importance

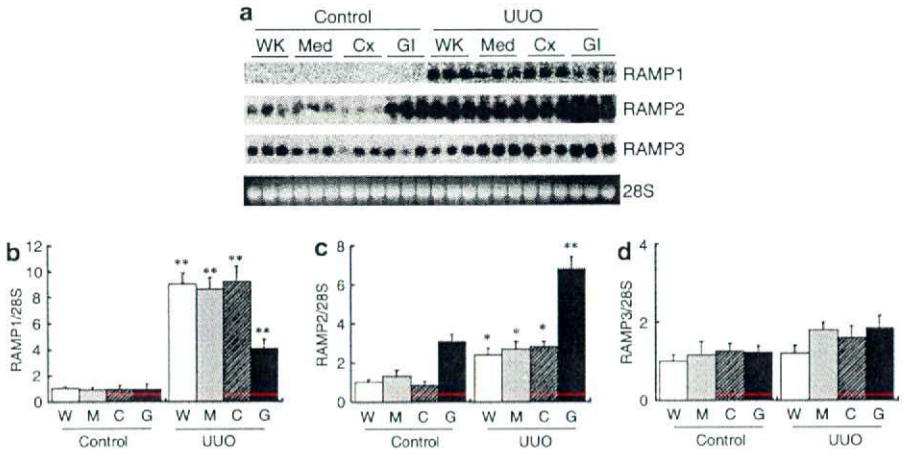

Figure 10 | Distribution of the *Ramp* family mRNA expression in UUO kidneys. (**a**) Distribution and changes of mRNA expressions of the *Ramp* family in the kidney after UUO. (**b–d**) The relative mRNA levels of *Ramp's* normalized with 28S ribosomal RNA in the control and obstructed kidney at day 6. The expression levels in the whole kidney from control (sham operated) rats were defined as 1.0 arbitrary unit. WK or W, whole kidney; Med or M, medulla; Cx or C, cortex; GI or G, glomerulus. $^{*}P < 0.05$, $^{**}P < 0.01$ vs control. $n = 5$.

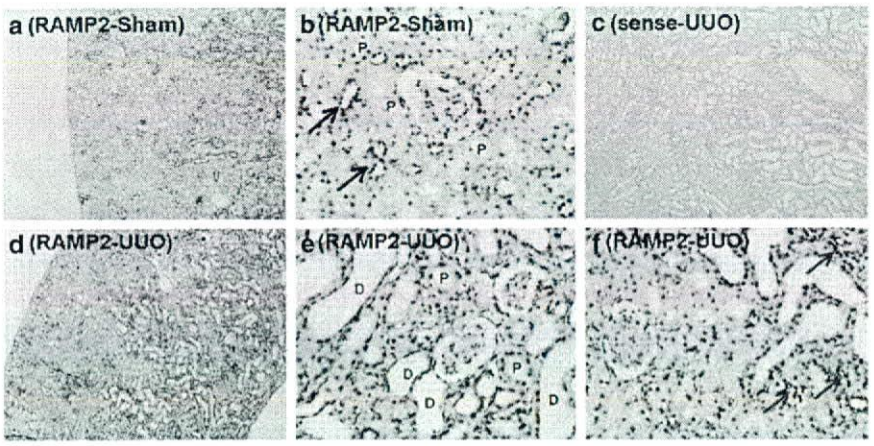

Figure 11 | Localization and changes of *Ramp2* mRNA expression in the kidney after UUO. (**a**, **b**) In sham-operated kidney, *Ramp2* was expressed in all nephron segments, such as glomeruli, proximal tubules (P), and distal nephrons (black arrows). (**c**) Control sense probe gave no signals in UUO kidney. (**d–f**) In UUO kidney, *Ramp2* was upregulated evenly in nephrons, and was newly induced in interstitium (red arrows) adjacent to dilated distal nephrons (D). Original magnification: × 40 (**a**, **c**, **d**) and × 200 (**b**, **e**, **f**).

of direct renal actions of ADM in modulating the pathophysiology of UUO.

In the process of renal interstitial fibrosis, renal fibroblasts play a key role by their involvement in the proliferation, migration, and synthesis of growth factors and matrix proteins.[31–33] ADM stimulates not only cAMP production but also calcium mobilization in cultured endothelial cells. The latter effects result in an increased nitric oxide production to enhance cGMP accumulation in the vasculature, thereby contributing to vasodilatory effects of ADM in concert with increased cAMP production.[11,12] In this study, we showed that ADM significantly suppressed TGFB1-induced upregulation of *Ctgf* and *Fn1* expression in NRK-49F renal fibroblasts. ADM as well as membrane-permeable analogs of cAMP and cGMP, both of which are intracellular signaling molecules of ADM, effectively abolished the upregulation of *Ctgf* and *Fn1* mRNA. Pretreatment with PKA inhibitor reversed this suppression, but neither protein kinase G inhibitor nor phosphatidylinositol 3-kinase inhibitor affected the response, demonstrating the critical role of the cAMP/PKA pathway in fibrogenesis of these cells.

Sustained activation of MAPK1/MAPK3 in renal tubular and interstitial cells in UUO provides a possible mechanism of the proliferative response against interstitial injury.[27] We and others have reported potent inhibitory effects of ADM on mesangial cell proliferation,[10,34–37] but little is known about the antiproliferative action of ADM on tubulointerstitial cells *in vivo* and *in vitro*. The present study revealed that the tubulointerstitial proliferation was attenuated in the kidney overexpressing *ADM* gene with the inhibition of MAPK1/MAPK3 phosphorylation.[24] Furthermore, ADM decreased PDGF-induced thymidine incorporation and MAPK1/MAPK3 phosphorylation in NRK-49F cells, consistently with a recent work reporting that ADM inhibited basal and EGF (epidermal growth factor)-stimulated proliferation in these cells.[38] Because interstitial volume expansion in obstructed kidney has been attributed to fibroblast differentiation/proliferation and extracellular matrix deposition,[39] the suppressive effects of ADM on the increasing renal mass of the ligated kidney are likely the results of antiproliferative and antifibrotic effects of ADM on renal fibroblasts. Interestingly, suppression of CTGF activity in UUO by introduction of antisense oligonucleotide through renal vein only inhibited fibrotic changes but did not affect renal cell proliferation,[6] although overexpression of *ADM* via a similar route in this study reduced both tubulointerstitial fibrosis and proliferation. These findings highlight the potentially distinct effects of the future strategy to treat fibrosis-associated renal diseases either by CTGF blockade or by ADM administration. We and others have shown that ADM possesses a potent inhibitory activity against oxidative stress, which may also play a role in its antifibrotic effects described in the present study.[22,23,40,41]

In the UUO kidney, cAMP production rate was enhanced, which was partially blocked with ADM-neutralizing antibody. We show here that *Ramp2* expression is upregulated in the obstructed kidney, and that overexpression of *Ramp2* and *Calcrl* reconstitutes a functional rat ADM receptor. Therefore, we propose that upregulation of *Ramp2* expression plays an important role in the activation of the endogenous ADM–ADM receptor system in UUO, and this may augment the protective effects of exogenous *ADM*.

Furthermore, we investigated renal localization of rat *Adm*, *Ramp2*, and human *ADM* by *in situ* hybridization. Exogenous human *ADM*, introduced by retrograde adenovirus infection via renal vein, was expressed predominantly in the interstitium. In a previous report, it was demonstrated that the gene delivery method used in this study specifically targets interstitial fibroblasts, and spares endothelial cells and proximal tubules.[26] Despite highly localized expression, exogenous *ADM* exerted potent protective effects upon both tubular and interstitial cells. This may be explained by possibilities that the gene delivery enhanced secretion of protective factors (including ADM) and, at the same time, suppressed release of deteriorating factors (such as CTGF) from renal interstitium, and that these soluble factors acted in paracrine manners. We also found that, in UUO kidneys, *Ramp2* expression was upregulated along all nephron segments and was also induced in the interstitium. Overexpression of exogenous *ADM* in interstitium did not reflect a physiologic response to UUO (because we did not find upregulation of endogenous rat *Adm* in the interstitium), but turned out to be an excellent strategy to carry out gene therapy.

In summary, we demonstrate here that adenovirus-mediated *ADM* gene delivery into the kidney ameliorates the histologic alterations caused by UUO. The results also suggest that the renoprotective effects of *ADM* in tubulointerstitial proliferation and fibrosis are not due to systemic blood pressure reduction, but due to cAMP-dependent CTGF suppression and inhibition of MAPK1/MAPK3 phosphorylation. These findings indicate that ADM may offer a new therapeutic strategy to prevent renal fibrosis in obstructive nephropathy and perhaps in other chronic nephropathies leading to tubulointerstitial fibrosis.

MATERIALS AND METHODS

Materials

Human ADM and CALCA (CGRP) were obtained from Peptide Institute (Osaka, Japan). 8-Bromo-cAMP and 8-bromo-cGMP were from Sigma (St Louis, MO, USA), and Rp-cGMP (final 10 μM) was from Biolog (La Jolla, CA, USA). Rp-cAMP (10 μM), myristoylated PKA inhibitor amide 14–22, and LY294002 were purchased from Calbiochem (San Diego, CA, USA).

Construction of recombinant adenovirus

Recombinant adenovirus encoding human *ADM* cDNA was synthesized by COS-TPC method[42] using Adenovirus Expression Vector Kit (Takara Shuzo, Otsu, Japan). Briefly, human *ADM* cDNA (nucleotides (nt) 124–737) containing the complete coding region of *ADM*[7] was ligated into cosmid cassette vector pAxCAwt, which contains the CAG promoter consisting of cytomegalovirus immediate early enhancer and chicken β-actin/rabbit β-globin hybrid